Physics – Uspekhi **58** (2) 167 – 190 (2015)

INSTRUMENTS AND METHODS OF INVESTIGATION PACS numbers: 41.20.Jb, 42.25.Bs, 42.30.Wb, 43.20.Gp

Experimental realization of invisibility cloaking

A V Shchelokova, I V Melchakova, A P Slobozhanyuk, E A Yankovskaya, C R Simovski, P A Belov

DOI: 10.3367/UFNe.0185.201502e.0181

Contents

Abstract. Advances in the studies of metamaterials have pushed the development of invisibility cloaks, which suppress scattering by objects within certain frequency ranges. During recent years, there has been a transition from a purely theoretical consideration of the cloaking effect to its practical implementation. This paper is an overview of the current state of the art in the area of invisibility cloaks. Special emphasis is put on experimental realizations of such devices.

Keywords: invisibility, cloaking, transformation optics, metamaterials, scattering cancellation, optical illusions, carpet invisibility cloak, active cloaking

1. Introduction

Invisibility and cloaking have been treated as science fiction for a long time [1–3]. However, this field of physics currently evolved into the subject of wide speculation on the part of the global scientific community, which is proved by the constantly growing number of publications. Significant increase of interest in the science and technology of invisibility cloaking is explained by the discovery of metamaterials in the early 21st century [4–17].

But what are invisibility and invisibility cloaks? In this article by invisibility we mean a situation when the object does not scatter or absorb the incident electromagnetic radiation in a specific frequency range. Strictly speaking, the invisibility of the object is the absence of electromagnetic field perturbations around the object at large enough distances from it.

As is well-known, the difference in the electromagnetic field distributions in the presence of an object and its absence is requisite for detecting the object [18]. By this means, neither the object may not reflect an electromagnetic wave in the opposite direction, absorb and scatter it in side directions nor the wavefront of an incident electromagnetic wave has to be completely recovered after having passed through the object to be hidden, i.e., to become similar to a wave propagating in vacuum, if an ideal invisibility is to be achieved. In terms of the theory of light scattering by this is mean that in the ideal case the total scattering cross section σ has to vanish at any frequency within the boundaries of a given frequency range.

The devices or coatings that allow achieving the invisibility of objects to be hidden we will call *invisibility cloaking devices or cloaks*. An ideal 'invisibility cloak' has not been designed yet and, actually, the possibility of producing such a system raises serious concerns [18–20]. However, due to the fast development of new fields of physics, such as the physics of metamaterials, transformation optics [21], and plasmonics [22, 23], it has become possible to manufacture cloaks which significantly reduce the scattering of the incident electromagnetic radiation by the object. But still, these materials operate in a rather narrow frequency range and only with motionless or low-speed objects.

It should be noted that our definition of invisibility does not include natural camouflage which is the ability of some living organisms to adapt their coloration or properties to the environment.

A V Shchelokova, I V Melchakova, A P Slobozhanyuk, E A Yankovskaya, P A Belov St. Petersburg National Research University of Information Technologies, Mechanics and Optics, Kronverksky prosp. 49, 197101 St. Petersburg, Russian Federation
E-mail: alena.schelokova@phoi.ifmo.ru, melchakova-i@yandex.ru, a.slobozhanyuk@phoi.ifmo.ru, adfors@gmail.com, belov@phoi.ifmo.ru
C R Simovski St. Petersburg National Research University of Information Technologies, Mechanics and Optics, Kronverksky prosp. 49, 197101 St. Petersburg, Russian Federation; Aalto University, School of Electrical Engineering, P.O.Box 15500, FI-00077, Aalto, Finland. E-mail: konstantin.simovski@aalto.fi

Received 4 February 2014, revised 12 May 2014
Uspekhi Fizicheskikh Nauk **185** (2) 181 – 206 (2015)
DOI: 10.3367/UFNr.0185.201502e.0181
Translated by A L Chekhov; edited by A Radzig

Naturally, invisibility cloaking is important for military applications. Due to this fact, achievements in the field of antiradar masking should be noted. The Soviet physicist P Ya Ufimtsev published in 1962 the book Edge Wave Method in the Physical Theory of Diffraction [24] which initiated the development of so-called stealth technologies aimed at making new types of arms (tanks, airplanes, missiles, satellites, ships, etc.) with low radar visibility. The developer of an object which must be protected from radar with stealth technologies has to minimize the back scattering (in the direction of the radar beam). This can be achieved by designing the object's form in such a way that the wave incident on the object may not be reflected in the opposite direction, but is either partially scattered in other directions or partially absorbed [25]. However, stealth technologies have a significant disadvantage: they lose their efficiency if the radar system consists of two and more spatially separated radars.

Invisibility cloaks operating in the radar frequency band have an advantage over stealth coatings, because they weaken the radar radiation scattering in all directions instead of only the opposite one.

Today, there are a large number of different cloaking methods, but one can distinguish the two most developed techniques:

(1) cloaking based on the wave flow method (Fig. 1a);

(2) cloaking based on scattering cancellation (Fig. 1b).

The invisibility achieved by *cloaking based on the wave flow method* is realized in the following way. The object is placed in a shell which causes electromagnetic fields to bend around the object and to recover their wavefront and intensity distribution afterwards. The operation of such a shell does not depend on the properties of the hidden object, because in this case electromagnetic waves do not interact with the object.

Cloaking based on scattering cancellation is realized when the scattering from the object and from the special coating compensate each other, and the radiation propagating through an object is not influenced by the latter. In this case, the properties of the invisibility cloak depend on the properties of the hidden object. When the object absorbs radiation, one has to use active materials or inner sources in the coating in order to fully compensate the scattering.

Besides the two invisibility techniques mentioned above, there are other methods as well, for example, so-called active cloaking [26], external cloaking [27], and cloaking based on a transmission-line network [28]. There are reviews in Russian publications devoted to invisibility and cloaking of objects [18, 21, 29–31], in which information about all known theoretical principles of optical invisibility can be found.

The goal of this article is to give a review of the most convincing *experimental realizations* of cloaks in various frequency bands. Therefore, we discuss in more detail the experimental realizations of cloaking materials based on wave flow and scattering cancellation methods. Section 4 concerns the most interesting, in our opinion, results of experiments based on other concepts producing invisibility effect.

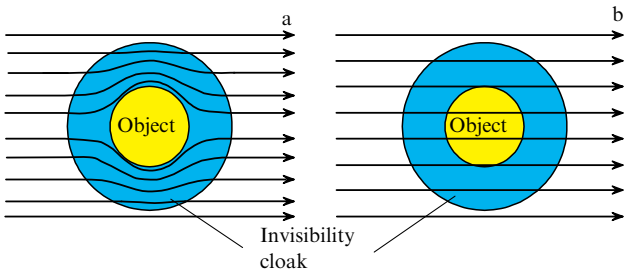

Figure 1. Cloaking based (a) on the wave flow method, and (b) on scattering cancellation.

2. Cloaking based on the wave flow method

2.1 Invisibility and cloaking based on the transformation optics

In recent years, a number of scientific teams have achieved success in metamaterial development. This opened significant opportunities in light flow control on both the microscopic and macroscopic scales. A field of physics has recently appeared — transformation optics — which allows looking at the fundamental laws of optics from a new angle, and creating new research areas in the science of light [21, 32–35]. One promising application for transformation optics is the development of cloaking devices.

Transformation optics relies on the fact that the Maxwell equations are invariant under the coordinate transformations if the material (electromagnetic) parameters of the media (usually, the permittivity tensor ε and the magnetic permeability tensor μ) also transform in a proper way [21]. An object (without cloaking) can be invisible in a homogeneous medium if its dimensions are negligibly small, because any object with a finite size would, of course, scatter the incident radiation. By performing a coordinate transformation that transforms a point object into an object with finite dimensions, it can be kept invisible if ε and μ have the proper distribution around it. Although transformation optics is a new line of inquiry in optics and materials science, invariant transformations of the Maxwell equations have been known even in the 20th century [36–42].

In this article, we will not discuss the theory of the wave flow method based on transformation optics: the theoretical aspects can be found in Refs [21, 29, 43]. We will only review the experimental realizations of cloaks, but before that, it is useful to make several comments.

First, one needs to realize the appropriate distributions of ε and μ over the thickness of the coating, which are calculated using the mathematical apparatus of transformation optics. This cannot be done by using materials that occur in nature, because they cannot provide the needed set of material parameters. One needs metamaterials with predefined electromagnetic parameters, which can be designed by synthesizing arrays of structural elements (particles). The structural elements of the metamaterial are usually resonant metal elements. Depending on the chosen operating range of the device, these elements can be split-ring resonators (SRRs) [44–46], canonical spirals [47, 48], pairs of plasmonic particles, plasmonic nanowires, and others. Metaatoms — metamaterial unit elements — can be made for the radio frequency band from an insulator with high permittivity [49]. The first experimental cloaking devices based on transformation optics were realized in the microwave frequency range [44]. Attempts to design infrared (IR) and visible band devices were made later.

Second, in order to develop cloaking materials based on transformation optics, highly inhomogeneous metamaterials with extremely high anisotropy and low optical losses are needed, which is very hard to realize in practice. Therefore,

developers have to find a compromise between the ideal ε and μ distributions and the realizable ones. This compromise can be achieved by replacing the requirements of full invisibility with partial invisibility requirements, for example, by considering two-dimensional optical cloaking or by abandoning some other conditions, like narrowing the frequency band or decreasing the size of the hidden object.

It is the absence of limitations on the size of the object to be cloaked that assures one of the main advantages of cloaking based on transformation optics. As was mentioned above, this is directly connected with the most precise realization of the ideal spatial distributions of ε and μ tensors, and these tensors must be strongly anisotropic, with their components having a small imaginary part. In actual practice, the required anisotropy can be achieved only for radio frequencies in a narrow band, for example, in the microwave band.

As for the optical losses, all known bulk metamaterials exhibit high resonant losses. The existence of losses is the main factor that lowers the efficiency of experimental realizations of cloaking materials based on transformation optics. Currently, the most common solution to the losses problem reduces to using an amplifying medium. However, practical success in this area is quite poor [50].

2.1.1 Practical realizations of cloaks. *Cloaking devices based on split ring resonators.* The pioneering work [44] published in 2006 demonstrates the first experimental realization of a metamaterial-based two-dimensional cloaking device that operates in the microwave range. The object to be cloaked was a copper cylinder with a diameter of about 1.4λ, where λ is the operating wavelength (the cloaking device was extremely narrowband). The experimental mock-up of the cloaking device, shown in Fig. 2, consisted of 10 concentric cylindrical layers of insulator, which split into elementary cells (with 3 cells arranged vertically) with metaatoms from SRRs. The experiment was performed in a parallel-plate waveguide at

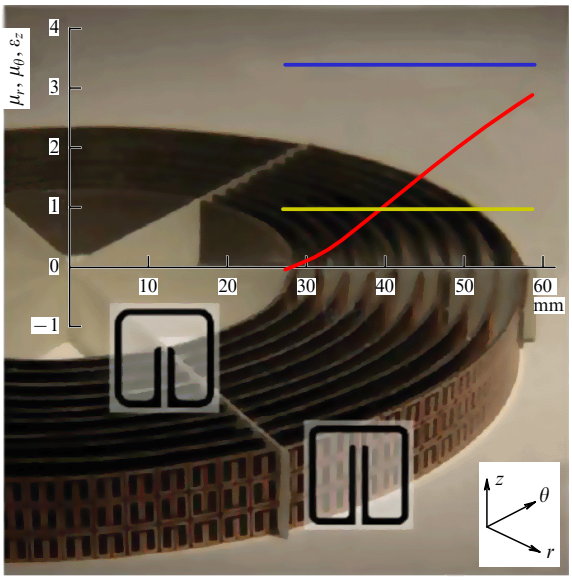

Figure 2. (Color online.) Two-dimensional cloaking device operating in the microwave wavelength band and graphical representation of the realized values for the material parameters: μ_r (red line), $\mu_\theta = 1$ (yellow line), $\varepsilon_z = 3.423$ (blue line), where r, z, θ are radial, vertical, and angular coordinates, respectively [44].

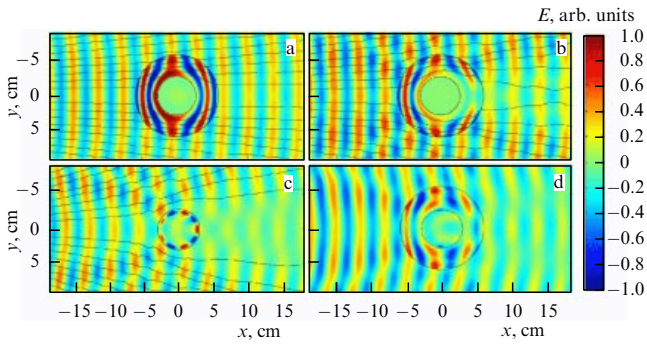

Figure 3. (Color online.) Distribution of the electric field strength: (a) numerical modeling for a cloaking device with an ideal distribution of the electromagnetic parameters of the medium; (b) numerical modeling for a cloaking device with simplified structural parameters; (c) experiment with a cylinder without cloaking device, and (d) experiment with a cylinder in a cloaking shell [44]. Color bar on the right-hand side of the figure shows the normalized instantaneous value of the electric field strength.

8.5 GHz frequency for a TE-polarized wave. The variation of electromagnetic parameters ε and μ was achieved by varying the SRR geometry.

Figure 3 gives the results of calculations and measurements of the electric field strength distribution, when the wave is incident from the left side on the conducting copper cylinder (shown as a circle in the center of every figure). The ring area around the cylinder stands for a cloaking device (metamaterial shell); solid lines in Figs 3a and 3b indicate the local directions of the energy flow. The field complex amplitude measurements were performed by using a special point-probe, which had practically no effect on the local electric field. The cloaking device reduces both the back scattering (reflection) and forward scattering. The cloaking device was assembled using a simplified homogenized model for the parameters and also had resonant losses in the metamaterial; therefore, the achieved masking was not close to the ideal one.

In 2010, the scattering cross section was measured for an object hidden in the cloaking shell under discussion [45]. It turned out that the scattering reduced by only 24%. Therefore, work [44] has only historical significance as the first practical demonstration of the invisibility concept based on transformation optics.

Experimental investigations with a similar scale model of the cloaking device were performed by Russian scientists as well [51]. The authors developed an automated measuring system which allowed obtaining an image of the spatial distribution of the electric field components. The measurements were performed in a broad frequency band, from 7 to 12 GHz, and the maximally possible cloaking effect was demonstrated at specific frequencies.

Another experimental demonstration of a two-dimensional nonmagnetic cloaking device for the microwave frequency band, based on electric SRRs, was presented in 2009 [46]. The cloaking device consisted of 15,700 SRR in silicon frames. The sample had a cylindrical housing, which was split into 20 ring regions with a linear variation of ε along the radial coordinate from the inner to the outer boundaries of the device (Fig. 4a). The inner radius of the sample was 6 cm, and the outer was 15 cm. The scheme of the experimental setup is shown in Fig. 4b. The system was excited with a horn antenna and the near field on the lower side of the cloaking device was scanned with a magnetic probe. The frequency of 11 GHz was chosen as the operational one. The experimental

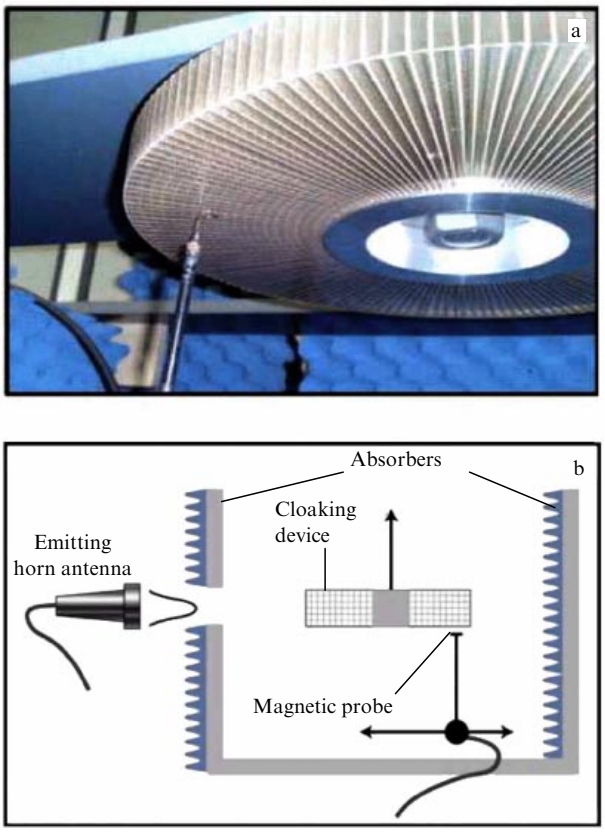

Figure 4. Nonmagnetic metamaterial device: (a) photograph, and (b) schematic of the experimental setup [46].

results are demonstrated in Fig. 5. Researchers succeeded for the first time in hiding a region of size 4.4 λ.

Theoretically, this approach to creating a two-dimensional cloaking device can be generalized to the case of the IR and visible bands, replacing TE-polarized waves with TM-polarized ones. In this case, one should replace magnetic metaatoms — SRRs — with optically short nanowires [52]. However, there have not yet been any experimental implementations.

Cloaking devices based on canonical spirals. The authors of Ref. [47] suggested a two-dimensional cloaking device based on so-called canonical spirals, shown in Fig. 6. A canonical spiral is a split ring with two segments of wire on both edges of the slit that are perpendicular to the plane of the ring. The needed realization of electromagnetic parameters can be achieved simultaneously for ε and μ only by utilizing one type of elements — spirals. The induced current in the spiral produces an electric dipole (due to the wire) and a magnetic dipole (due to the ring). The cloaking device is split into concentric cylindrical regions (layers) with canonical spiral inclusions. The needed radial variation of the permittivity in this cloaking device is achieved by varying the spatial density of the location of spirals possessing similar geometric parameters as a function of distance to the center of the cloaking device, while in previously discussed works this was achieved by using resonant elements with different parameters. Using spirals of the same size simplifies the manufacturing of the device.

This cloaking device can operate in free space only if the parasitic material parameter of the spiral-based metamaterial — so-called chirality — is compensated. Chirality describes

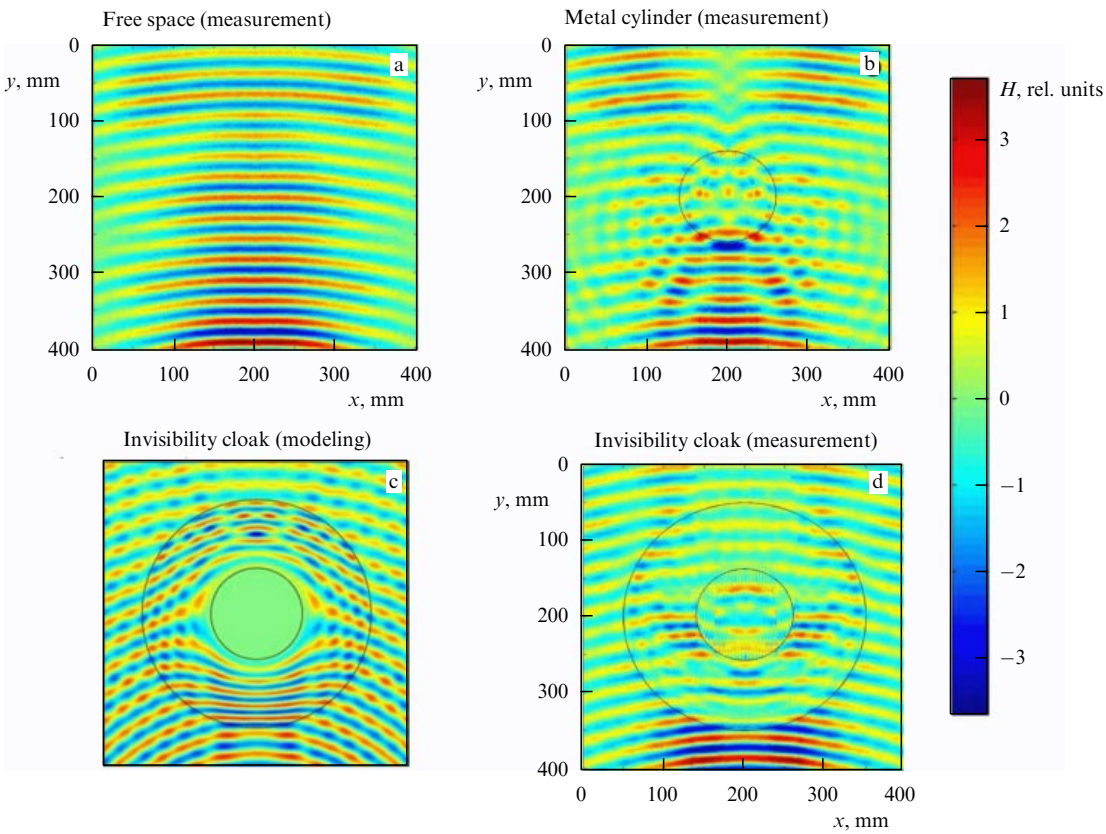

Figure 5. (Color online.) Real part of the measured magnetic field: (a) in free space; (b) only with the metal cylinder, and (d) with the metal cylinder in a cloaking shell. (c) Numerical modeling results for a metal cylinder in a cloaking shell. Operating frequency is 11 GHz, and waves propagate upwards [46].

Figure 6. Experimental mock-up of a cloaking device based on canonical spirals [47].

the electric-field-induced magnetic polarization and the magnetic-field-induced electric polarization of the metamaterial unit volume. The chirality is compensated for by tapping the same amount of right-hand and left-hand spirals in the cloaking device. Such a two-dimensional cloaking device operates for low-height cylindrical objects with incident waves propagating in a horizontal plane. However, this two-dimensional cloaking shell has advantages over many other two-dimensional cloaking devices: it operates both for TE- and for TM-polarized waves and is easy to fabricate.

The authors used a metal cylinder 3 cm in diameter and 1 cm in height as an object to be hidden. The modeling and the experiment were performed at a frequency of 8 GHz for a cylinder without a cloaking shell and a cylinder with a cloaking shell. The results of the experiment performed in a parallel-plate waveguide are presented in Fig. 7. As follows from the results obtained, partial invisibility was achieved. Although the cloaking shell does not reduce the reflection, the shadow region behind the cylinder, placed in the center of the cloaking device, is much smaller than the shadow of the cylinder without a cloaking device. Moreover, almost full wavefront recovery is observed behind the hidden cylinder, while the enhancement in the reflection, predicted by the numerical model, is not observed experimentally. In order to increase the efficiency of this cloaking device, the density of the canonical spirals needs to be increased in every layer.

2.1.2 Carpet cloaking. As mentioned above, there are no theoretical limitations on the size of an object hidden with an invisibility cloak based on transformation optics. But it is quite hard to technologically realize in practice the materials with the required distribution of the electromagnetic parameters for their operating in a broad frequency range, especially in the optical one. Therefore, a new cloaking method was suggested in article [53], which is based on transformation optics and wave flow — the 'transparent carpet' invisibility (Fig. 8).

In 'carpet' cloaking, the object to be hidden is placed on a highly reflecting surface and is covered with a layer that forms a transparent invisibility cloak. Then, the object appears as it were an asperity on the reflecting surface. It is enough to suppress the scattering from this surface irregularity in all directions, except for the specular one. There is no need to suppress the wave in the specular direction, but it has to be the

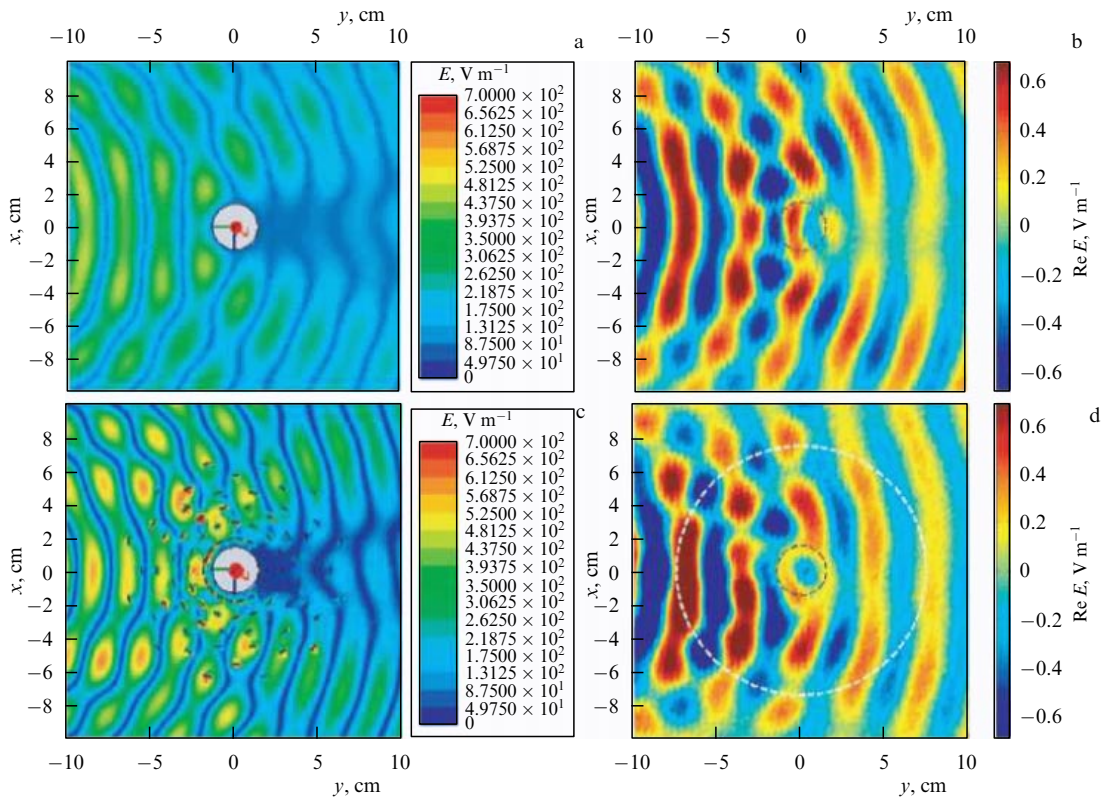

Figure 7. (Color online.) Numerical modeling of the electric field amplitude for a copper cylinder (grey circle): (a) without a cloaking device, and (b) with a cloaking device based on spirals. Measurement data for the real part of the electric field for a metal cylinder: (c) without a cloaking device, and (d) in the spiral cloaking device. Black dashed line indicates the cylinder surface, and the white one marks the outer boundary of the cloaking shell [47].

same as if it were reflected from the mirror substrate. It turns out that in this case the structure of the cloak can be simplified; namely, superstrong optical anisotropy is not needed and, moreover, a completely isotropic material can be employed.

The material parameters and shape of the carpet cloak are calculated applying the mathematical apparatus of transformation optics. Besides the fact that this type of cloaking can be performed with an isotropic medium, there is no need to use resonant metaatoms in its realization. Therefore, for cloaking materials that are invoked in a transparent carpet cloaking, there are no problems with high optical losses or a narrow frequency range. Carpet cloaking can also be applied for nonpolarized light. The most significant experimental results for such invisibility cloaks have been achieved in the microwave [54], terahertz [55], and optical [56] frequency ranges.

Carpet cloak devices in the microwave band. Paper [54] suggests a cloak made from more than ten thousand I-shaped particles with different parameters. Lattices of such particles form metamaterial layers with different effective refractive indexes and surface impedances (Fig. 9). Figure 10 presents the results of electric field measurements. Due to experimental equipment limitations, the measurement was only performed in the frequency range from 13 to 16 GHz, although the authors claimed that the frequency range where the cloaking effect can be observed is broader.

In 2011, an experiment [57] was carried out on creating a carpet invisibility cloak from polyurethane foam supplemented with barium titanate, the concentration of which changed with the vertical coordinate (Fig. 11). The experiment was performed in a parallel-plate waveguide in the frequency range from 7 to 12 GHz (Fig. 12). The main advantage of the chosen dielectric composite lies in the fact that it consists not of small subwavelength-sized components, but of units several dozen millimeters in size, so the

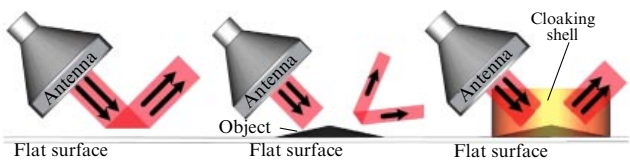

Figure 8. Operation principle of carpet invisibility cloak [53].

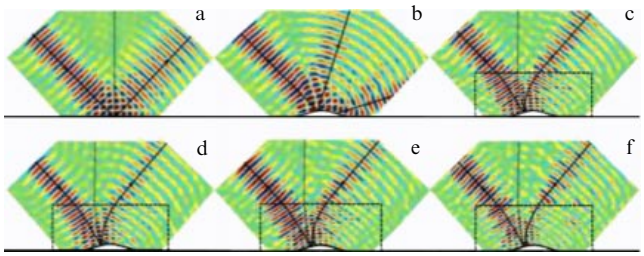

Figure 10. Experimental results of measuring the electric field distribution for a beam incident on a normal surface (frequency 14 GHz) (a), on a surface with an object without cloaking (frequency 14 GHz) (b), on a surface with an object under a carpet invisibility cloak at frequencies of 14 GHz (c), 13 GHz (d), 15 GHz (e), and 16 GHz (f). The fields in the reflected beam do not differ much from the fields in the beam reflected from the surface without the object [54].

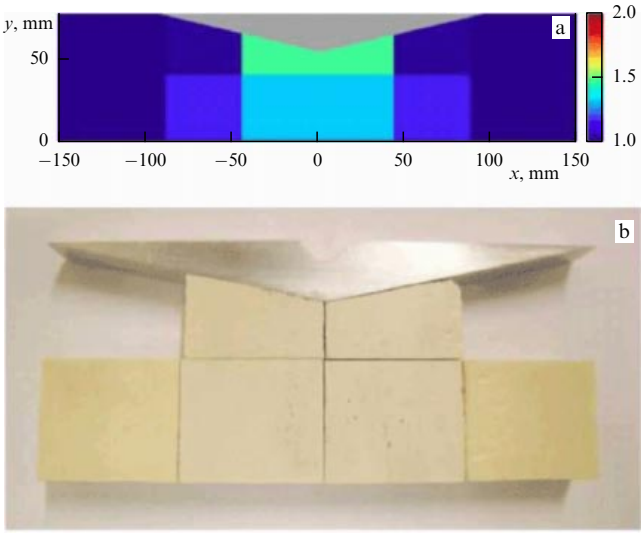

Figure 11. The object to be hidden confined by units of the composite dielectric with a spatially inhomogeneous distribution of barium titanate. The electromagnetic wave travels upwards. The object is an aluminum triangle 16 mm in height with a base of 144 mm. (a) Dielectric constant distribution of the units with dimensions 34.25 mm × 30 mm. (b) Exterior view of a fabricated device for carpet cloaking [57].

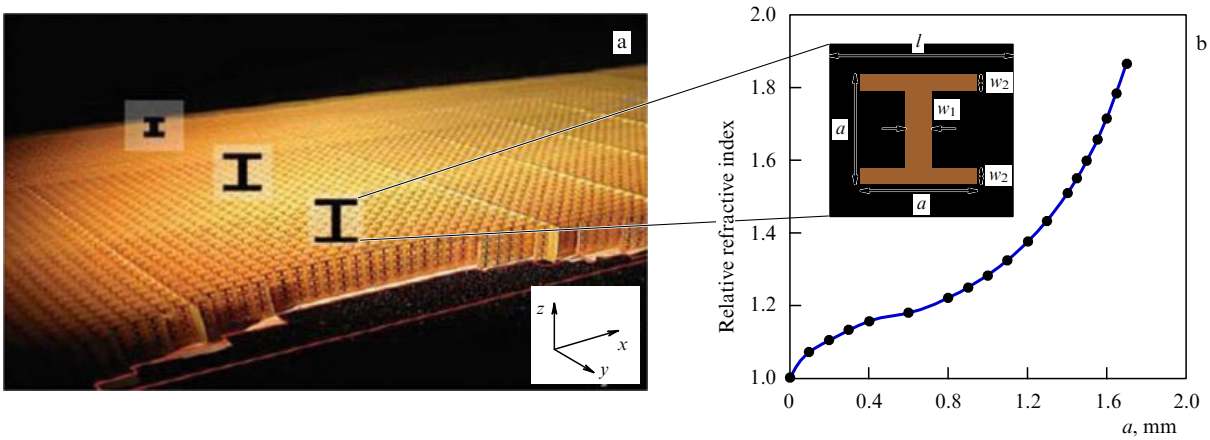

Figure 9. (a) Cloaking material model. (b) Refractive index versus the element size. The dimensions of the unit cell of the metamaterial are $l = 2$ mm, $w_1 = 0.3$ mm, $w_2 = 0.2$ mm; size a varies from 0 to 1.7 mm [54].

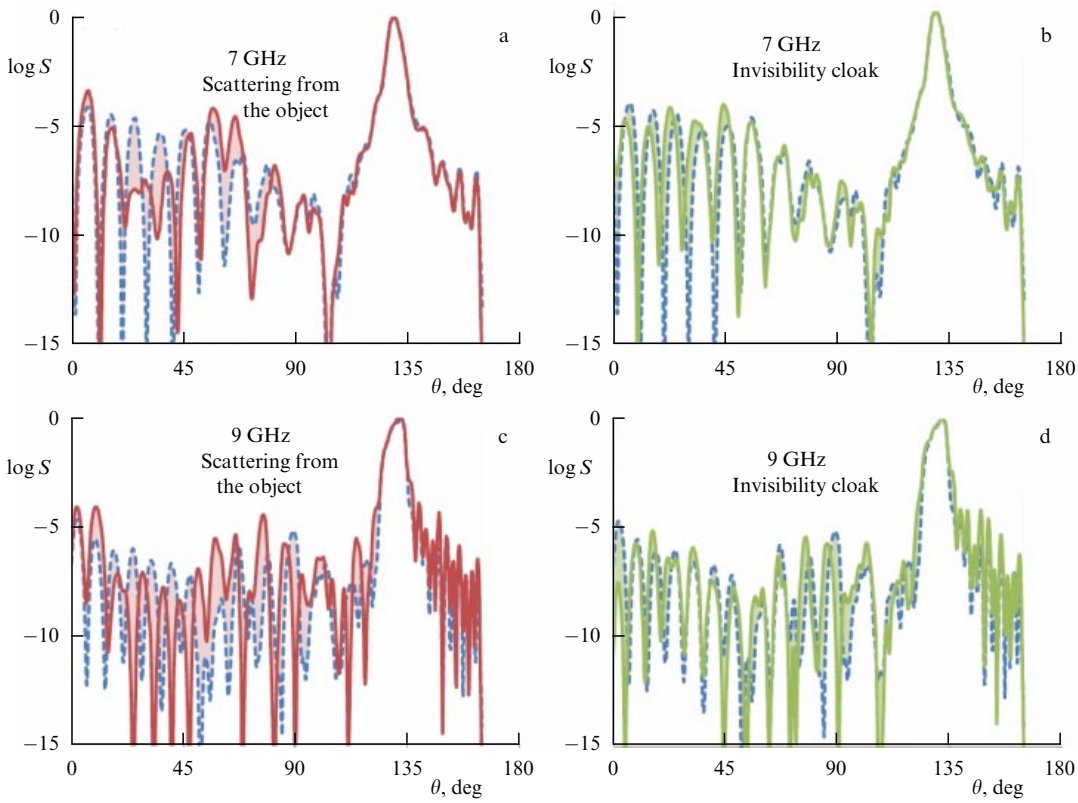

Figure 12. (Color online.) Experimental results: transmission coefficient S [dB] versus the wave angle of incidence θ. Scattering from the object (a, c) without an invisibility cloak (red line) and (b, d) with an invisibility cloak (green line). Dashed lines correspond to the scattering in an empty parallel-plate waveguide [57].

structure exhibits low losses and, at the same time, is easy to fabricate.

The carpet cloaks discussed above operate only in the case of a TM-polarized incoming electromagnetic wave. A three-dimensional carpet coating that operates for both polarizations was realized experimentally in 2010 [58]. The invisibility cloak was developed utilizing known dielectric materials with refractive indexes from 1 to 1.63 in the microwave band. The sample was a cylinder of 51 mm height and 62.5 mm radius, made of layers of dielectric plates with inhomogeneous holes (Fig. 13). The plates were manufactured from polytetrafluoroethylene and fiberglass with a relative dielectric constant of 2.65. The height of the plates was 1 mm. A cone-shaped metal object with a base radius of 62.5 mm and height of 13 mm was placed in the lower part of the cylinder. The experiment showed good results for both polarizations of the incident wave and different angles of incidence in a broad frequency range from 9 to 12 GHz (Fig. 14).

In the work discussed above [54, 57, 58], the parameters of the cloak were determined by the geometry of the object to be hidden, so if the object size or shape changes, one needs to develop a new cloaking device.

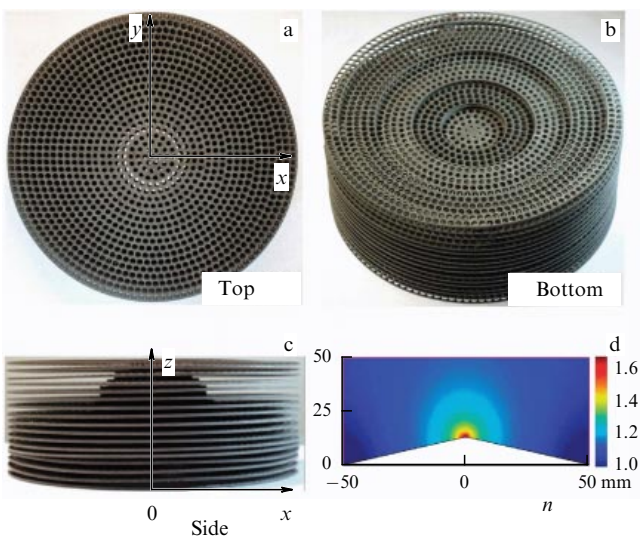

Figure 13. (Color online.) Experimental model of a three-dimensional device for carpet cloaking. Top view (a), bottom view (b), and side view (c). (d) Refractive index distribution in plane xz [58].

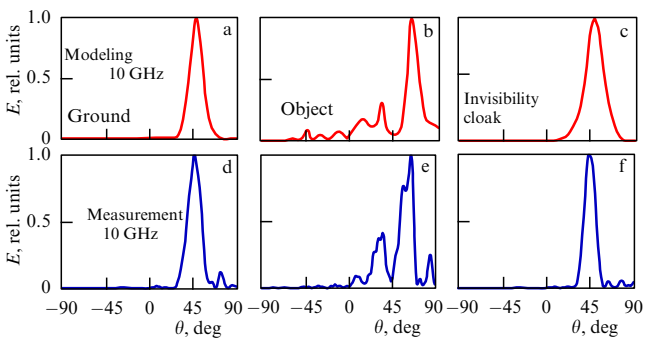

Figure 14. Theoretical (a–c) and experimental (d–f) results for the frequency of 10 GHz and TM-polarization; θ is the wave angle of incidence, and E is the electric field amplitude normalized to unity [58].

A new method of carpet cloaking was proposed in Ref. [59]. The authors suggested a new 'smart' metamaterial: a self-regulating metamaterial on the base of an elastic matrix with high permittivity. This metamaterial allows changing the size and shape of the region to be hidden. The possibility of experimental realization of invisibility carpet cloaking using this metamaterial was also confirmed in Ref. [59]. During the development of this metamaterial, the transformation optics apparatus was not applied: quasiconformal transformation of a homogeneous space with a point object into inhomogeneous space with a finite object was 'replaced' with the mechanical transformation of an elastic medium. Numerical modeling has shown that the best cloaking effect can be achieved by using auxetics — materials with a negative Poisson's ratio, in which the absolute value of the Poisson's ratio should be quite high. Currently, however, it is hard to realize a material with both high dielectric constant and negative Poisson's ratio. Therefore, the authors of Ref. [59] proposed a scheme which allows providing partial invisibility, while being quite simple in fabrication. The experimental sample of a 'smart' carpet cloak consists of two triangular parts (C_1 and C_2 in Fig. 15), each having an elastic crystal structure formed by empty silicone tubes pressed together. The lower triangular part is 'pressed' into the upper one; as a result, the silicone tubes experience deformation, which leads to the required distribution of ε in the cloaking shell. The region to be hidden also emerges, and its height can be controlled. Therefore, objects with different dimensions can be hidden.

As one can see from the results of the modeling and of the experiment (Fig. 16), the best cloaking effect is observed for small heights of the region to be hidden. As with other carpet cloak devices, smart cloaking operates in a broad frequency band from 10 to 12 GHz.

A significant breakthrough in carpet cloak design happened in 2012. Up to that time, all experiments had resulted in reaching only partial invisibility. Landy and Smith [60] developed a two-dimensional cloak that allowed them to achieve almost full invisibility of a cylindrical object for the microwave frequency band. The cloaking device has a diamond shape (Fig. 17) and contains two types of metaatoms: electric and magnetic particles that make it possible to obtain the necessary ε and μ distributions. The electric field vector of the incident wave is directed normal to the plane involving the cloak device, so the permittivity component ($\varepsilon_z = 2.36$) is out of the device plane, and the magnetic permeability components ($\mu_x = 3.27$, $\mu_y = 0.31$) lie in the plane of the device. The positions of the coordinate axes are

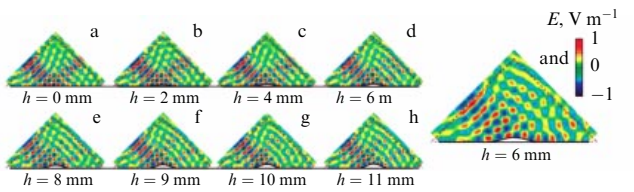

Figure 16. (Color online.) Experimentally obtained distribution of the electric field E at a frequency of 10 GHz: (a) for a cloaking shell without an object to be hidden, (b–h) for a cloaking shell with different heights of the region to be cloaked h, indicated in the figure, and (i) without a cloaking shell and with $h = 6$ mm. Red dashed line singles out the triangle corresponding to the boundaries of the carpet cloaking [59].

shown in Fig. 17a. The necessary electromagnetic parameters were realized with the aid of individual metamaterial inclusions — canonical double-sided SRRs (Fig. 17b). The magnetic and electric properties can easily be controlled by changing the length l_c of the capacitance arm and the height a_z of the unit cell, respectively. Such cloaking allows hiding a cylindrical object with radius $R = 7.5$ cm, placed in the center of the cloak device. An experiment in a parallel-plate waveguide at the frequency of 10.2 GHz demonstrated a reduction in the scattering from the object in a cloaking shell by ten times in comparison with the scattering from an object without cloak (Fig. 17c, d).

Nevertheless, invisibility in experiment [60] is, actually, partial, as it is in the other studies mentioned above, because it cannot be achieved for all the angles of a wave incidence. The operation frequency range, although it is broad, is still finite, and in most cases only one polarization of the incoming field is considered.

Carpet cloaks in the terahertz range. In 2011, a three-dimensional carpet cloak for the terahertz frequency range was suggested and experimentally realized [55]. The cloak (Fig. 18) has a triangular shape with an 8.52-mm base and 4.26-mm height and consists of 220 layers with holes of different diameters. A smooth 200-nm thick layer of gold was sputtered on the substrate, which plays the role of a mirror. The cloaking effect was observed at frequencies from 0.3 to 0.6 THz (Fig. 19).

Liang et al. [61] demonstrated in 2012 a cloaking device that consists of two mirror-symmetric sapphire prisms glued to each other. An object to be hidden can be placed in the triangular region with height $H_2 = 1.75$ mm, located under the prisms (Fig. 20). In order to test the device's operation, the

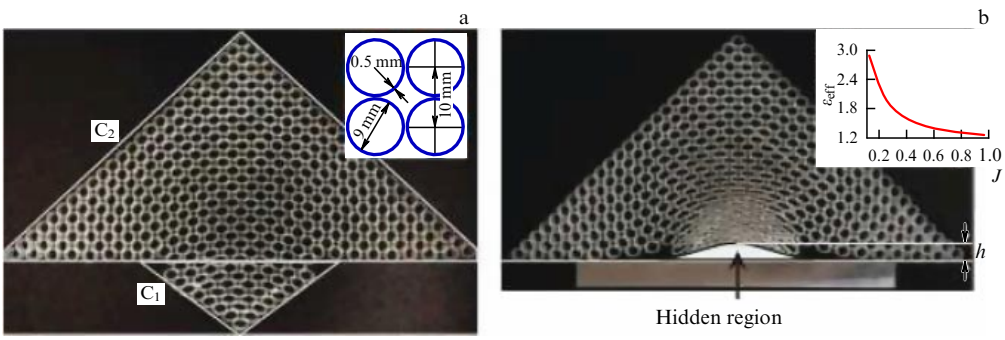

Figure 15. Experimental sample of a 'smart' metamaterial with an additional lower part (length 125 mm, height 65 mm): (a) before the deformation, and (b) after the deformation. Inset to figure (a) shows the geometrical parameters of the holes in the material, and inset to figure (b) plots the effective permittivity ε_{eff} versus the strain tensor Jacobian J which characterizes the compression (tension) and the shape variation at every point of the sample [59].

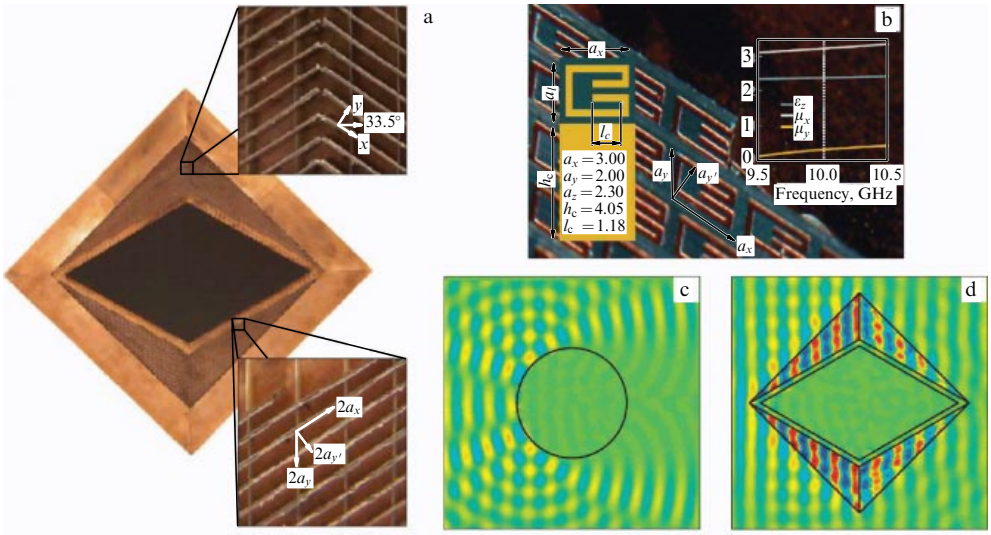

Figure 17. (Color online.) (a) Photograph of the experimental mock-up of a cloaking device with a length of about 41 cm. The square in the upper part of the figure corresponds to the inner surface of the cloaking device. White arrows indicate the local coordinate system. Corrugations are directed along the x-axis in order to obtain an effective response in this direction. The square in the lower part of the figure is a photograph of the material, with white arrows indicating the directions of the layer longitudinal vectors for a metamaterial unit cell. (b) The structure of the metamaterial unit cell. Inset to the left-hand side of the figure — schematic of the metamaterial unit cell; the dimension units are millimeters. Inset to the right-hand side of the figure — electromagnetic parameters versus frequency near the 10 GHz value. (c, d) Measurement results for the electric field at a frequency of 10.2 GHz for an original object and an object in the cloaking device, respectively [60].

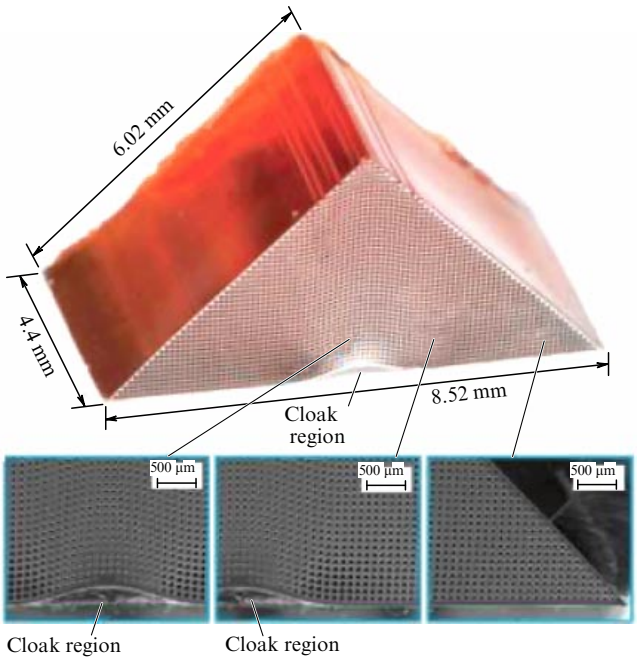

Figure 18. Model of a three-dimensional carpet cloak. Images obtained using optical and scanning electron microscopes. The surface was metallized in order to obtain a better resolution. The hole size variation is seen near the bump [55].

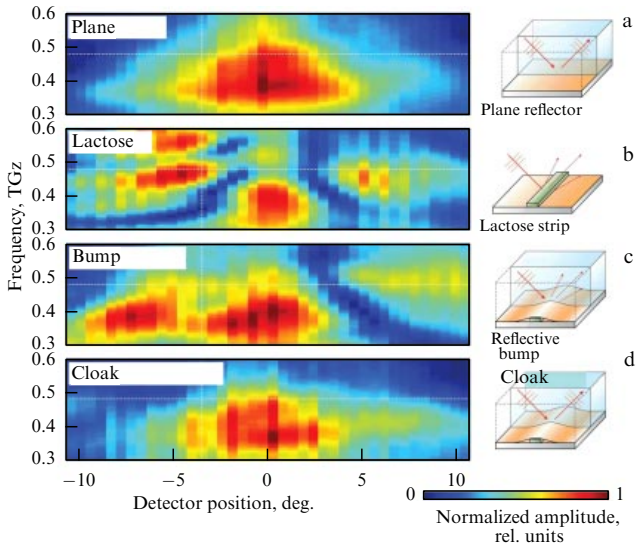

Figure 19. (Color online.) Spectra for four experimental cases: (a) reflective surface, (b) lactose strip — object to be hidden, (c) reflective bump, and (d) cloak [55].

authors measured the profiles of a terahertz beam that propagated through the cloaking shell. The beam was incident on one of the flat sides of the prism, while the profile was measured on the opposite edge. In this way, the results for TM-waves were obtained in the frequency range from 0.2 to 1 THz for incidence angles of $\pm 10°$ (Fig. 21).

Carpet cloaking in the optical range. The first realization of carpet cloaking at optical frequencies (in the IR range) was described in [62]. The cloaking shell is made on a laminated silicon-dielectric substrate, consisting of a layer of 250-nm-thick purified doped silicon, separated from the substrate with a 3-μm thick silicon oxide layer (Fig. 22). The role of an object is played by a bump on the mirror, formed as a gold stripe with a width of 250 nm and thickness of 100 nm, which limits the 250-nm silicon layer from the side. A cloak region is formed under the bump. Holes with a diameter of 110 nm are produced in the doped silicon layer, turning it into an anisotropic metamaterial for the near IR range. The cloaking shell is formed in the rectangular region around the bump on the mirror due to the fact that in this rectangle the same 110 nm holes are placed aperiodically with a proper spatial

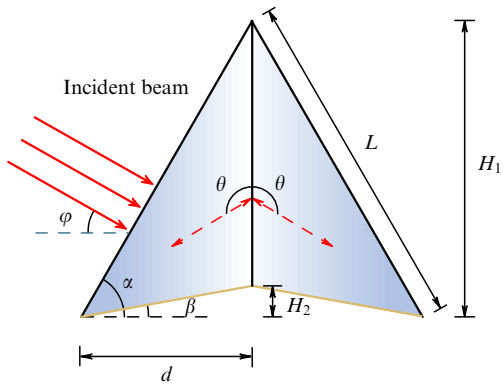

Figure 20. Schematic of the cloaking device geometry. The length $L = 40$ mm of the faces and the height $H_1 = 34.78$ mm form a lower angle $\alpha = 60.4°$. The angle to be hidden $\beta = 5°$. The optical axis of the crystal is directed at an angle $\theta = 58.5°$ [61].

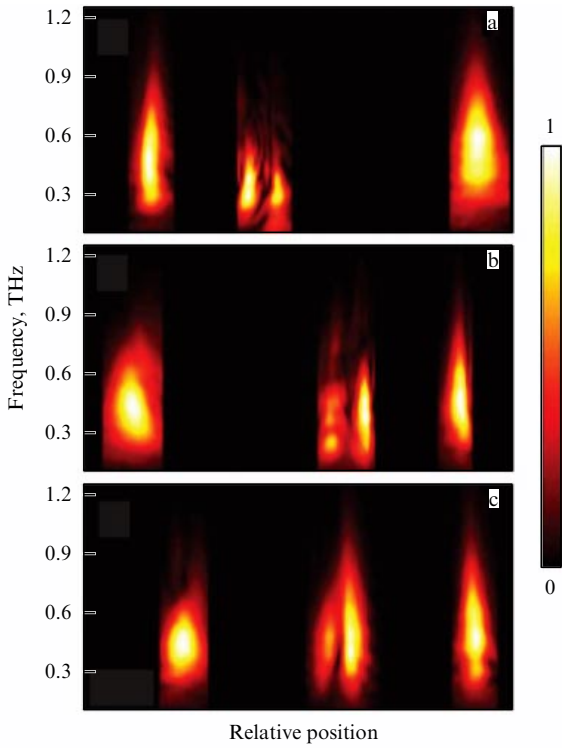

Figure 21. (Color online.) TE- and TM-profiles of a beam for the angles of incidence (a) $\varphi_1 = 19.6°$, (b) $\varphi_2 = 39.6°$, and (c) $\varphi_0 = 29.6°$ [61].

distribution. Such an invisibility cloak is two-dimensional — it operates in relation to waves propagating in a 250 nm silicon layer with the holes in the horizontal plane (as in a waveguide). Since this coating does not contain resonant metaatoms (holes can be treated as metaatoms that are not resonant), cloaking of good quality (Fig. 23) is observed in a quite broad wavelength range (1400–1800 nm).

A three-dimensional carpet cloak for the IR band was first developed in 2010 by Erkin et al. [56] and was based on dielectric face-centered cubic photonic crystals with a stacked structure (Fig. 24). The invisibility effect was observed for wavelengths from 1.4 to 2.7 μm, and at angles of incidence not higher than 60°.

In 2011, a two-dimensional carpet cloaking was simultaneously realized in several studies [63–65], being analogous to the one described in Ref. [62], but for visible light frequencies. In Ref. [63], such a cloak was made in a silicon–nitride waveguide on a specially designed nanoporous substrate from silicon oxide with a very low refractive index, $n \approx 1.25$ (Fig. 25). The cloaking device obtained demonstrates a broadband invisibility effect — almost for the whole visible light region (400–700 nm) (Fig. 26).

At the end of this section, let us note that cloaking based on transformation optics can also be adapted for screening from an external magnetic field, which was demonstrated in Refs [66, 67]. For these purposes, it was suggested to fabricate a cloak from a superconductor and a ferromagnet. In 2013, a 'heat cloaking device' was fabricated for the first time using coordinate transformation principles [68]. Such a device localizes the heat flow around the object in a metal plate, which minimizes the heating of the object. An improved model of this device was demonstrated in Refs [69, 70]. The first realization of a macroscopic cloaking device in the case of diffusive light scattering was also shown recently [71]. This device excellently hides the object at every angle of incidence of light and for any type of its polarization. Moreover, it can be useful to apply these principles in acoustics [72].

2.2 Invisibility and cloaking realizations without using transformation optics

2.2.1 Cloaking device based on a transmission-line network. An alternative way of invisibility cloaking was presented in Ref. [73]. It is based on the wave flow method but does not employ transformation optics. This method deals with a network of transmission lines (or long lines in terms of radio engineering) that are connected with each other. An electromagnetic wave incident from the environment on the cloaking

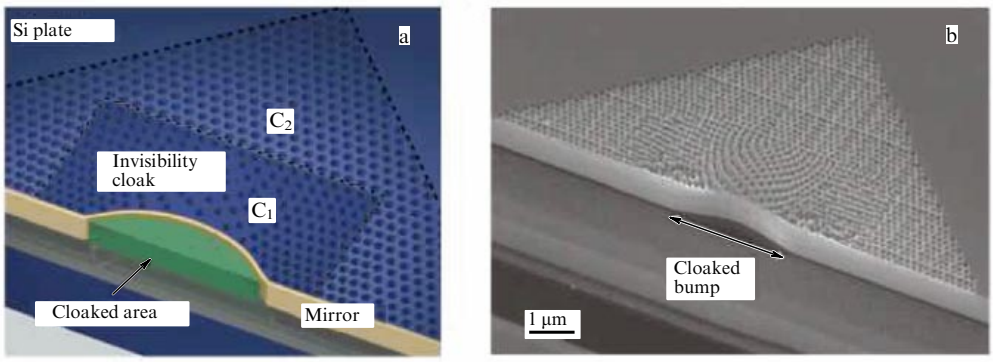

Figure 22. (a) Graphical model of a carpet cloak operating in the IR range. (b) Image of the carpet cloak obtained with a scanning electron microscope; the width and depth of the object to be hidden are 3.8 μm and 400 nm, respectively [62].

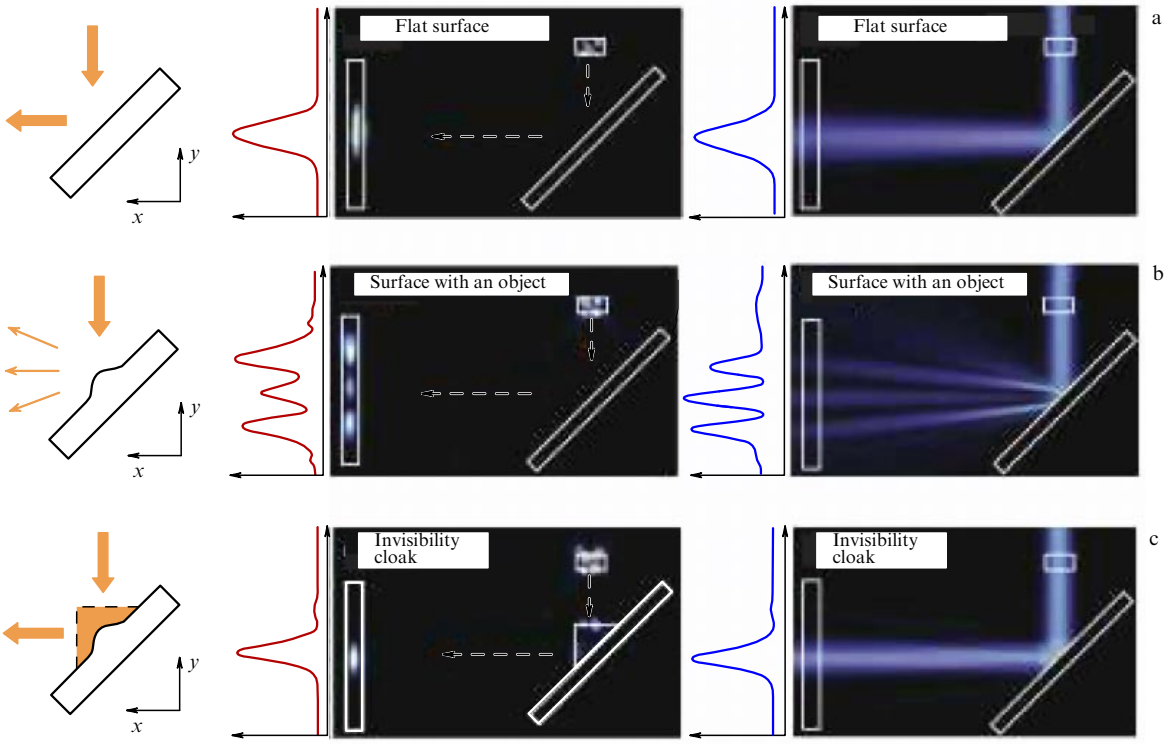

Figure 23. Experimental results for a reflected Gaussian light beam at a wavelength of 1540 nm for (a) a flat surface of the mirror, (b) a surface with a bump and with no cloaking, and (c) a surface with a bump and an invisibility cloak [62].

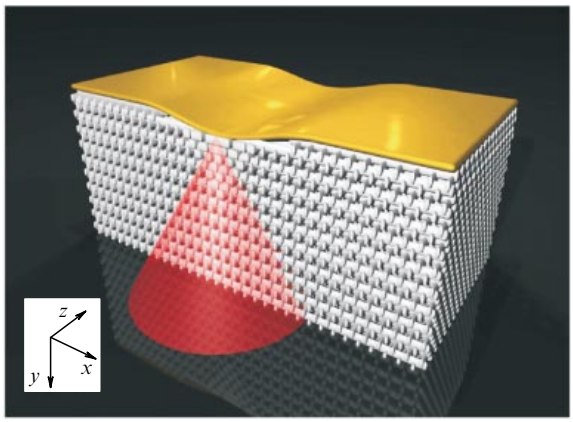

Figure 24. (Color online.) Model of a three-dimensional carpet cloak. The three-dimensional light cone, shown in red color, corresponds to the microscope numerical aperture NA = 0.5 [56].

device surface excites the transmission-line network which penetrates the object. The wave travels along the transmission-line network through the object in such way that it remains unnoticed both in the incident and in the transmitted or scattered fields (Fig. 27). If the size of the object to be hidden is much more than the wavelength, it needs either to have holes for the transmission-line network or to be a group of objects with a small lateral size, for example (in the two-dimensional case), a set of rods with diameters less than the network cell size.

In paper [74], a two-dimensional array of metal wires, which is a part of the cloaking device, was chosen as the object to be hidden (Fig. 28). The results of the experiment, performed in a parallel-plate waveguide, are presented in Fig. 29. Although the experiment was only concerned with the realization of two-dimensional invisibility based on the transmission-line network, it can also be realized, in principle, for a three-dimensional object with holes (or a three-dimensional cluster of small spheres) if the three-dimensional transmission-line network is realized.

This concept was further developed in Refs [75, 76]. The authors of this research improved the cloaking device by replacing its peripheral part with an array of hard conical metal layers. Conical layers play the role of a matching device, because the radial cross section of the conical layer can be treated as the longitudinal cross section of the horn antenna. The wave impedance changes smoothly in the conical layer, which allows almost completely suppressing the back scattering. The sample obtained of the invisibility cloak turned out to be the easiest one to fabricate and assemble. Moreover, its advantage is the possibility of performing measurements in free space. The object was a set of massive metal rods, connected to each other with metal rings, and the measurements were conducted using a horn antenna. The antenna directivity patterns in the case of free space and in the case of the object to be hidden in the cloaking device being in front of the antenna were almost the same. At the same time, the pattern changed significantly if the object was in front of the antenna with no cloaking. A schematic of the experimental setup and the results are shown in Figs 30, 31.

2.2.2 Cloaking device based on metal plates. Cloaking devices built around transmission lines are quite easy to realize and have a broad operation range, which, of course, makes them attractive for practical applications; but their main disadvantage lies in the existence of a limitation on the geometry of the object to be hidden. Another method of two-dimensional cloaking in the microwave and optical (IR) bands was

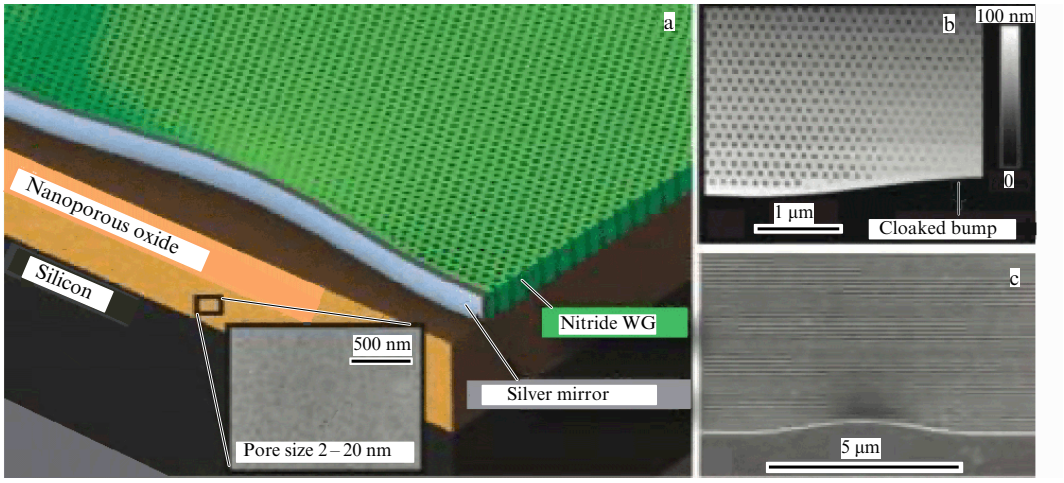

Figure 25. (Color online.) (a) Carpet cloak model, where the nitride layer thickness is 300 nm, the nanoporous oxide thickness ranges 5–10 μm, and the size of the holes varies from 20 nm to 65 nm. (b) Image of the holes was obtained with an atomic-force scanning microscope. (c) Image of the device that has around 3000 holes, obtained with a scanning electron microscope [63].

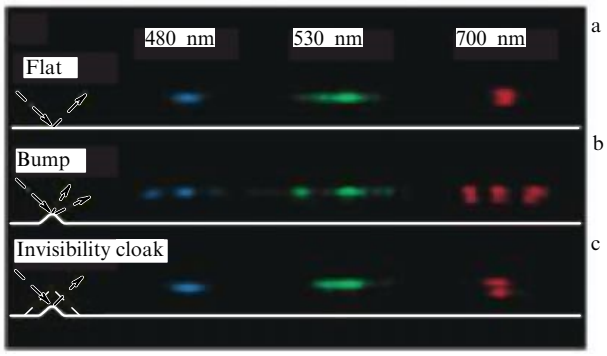

Figure 26. Experimental results obtained at various wavelengths: field intensity distributions after reflection from (a) a flat surface, (b) an object without an invisibility cloak, (c) an object with an invisibility cloak [63].

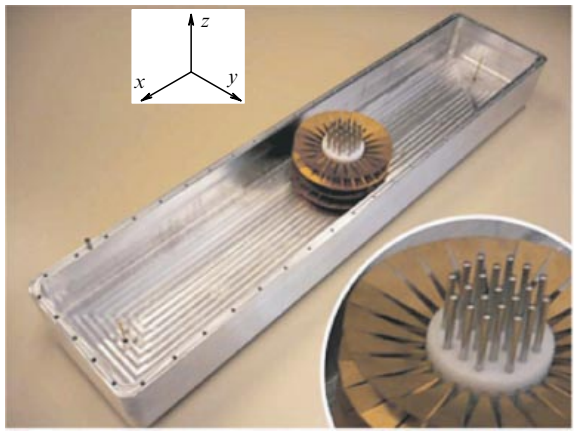

Figure 28. Photograph of a waveguide with an object to be hidden and a cloaking device [74].

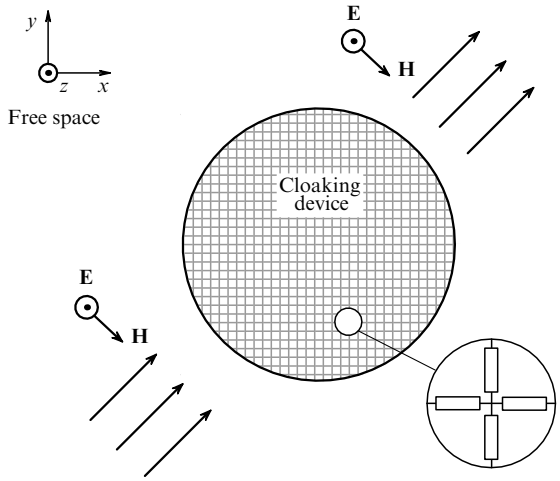

Figure 27. Two-dimensional cylindrical electromagnetic cloaking device. Its efficiency does not depend on the angle of incidence of the electromagnetic wave under the condition that the lattice period be small enough in comparison with the wavelength [73].

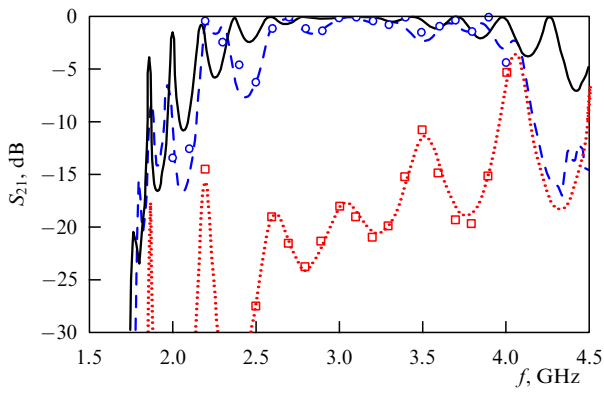

Figure 29. (Color online.) Transmission coefficient for an empty waveguide (black curve), for a waveguide with an object to be hidden in it (blue curve), and for a waveguide with an object to be hidden and a cloaking device (red curve) [74].

suggested in Refs [77, 78] — cloaking based on conical metal plates (conical metal layers). Unlike invisibility cloaks based on transmission lines, a cloaking device based on such plates can hide solid objects without a hole network.

The object to be hidden in paper [79] was a metal cylinder (made of copper for the microwave frequency range, and of silver for the optical one). The broadband electromagnetic cloaking device comprised a set of annular conical metal layers (Fig. 32). Along the vertical z-axis (the electric field is

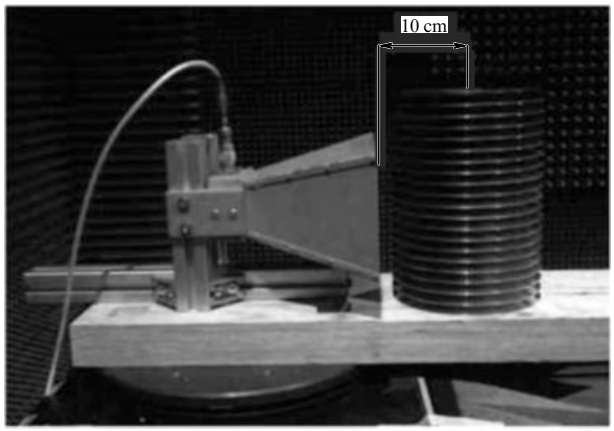

Figure 30. Mock-up of the experimental setup with an object to be hidden placed in front of a horn antenna [75].

assumed to be polarized along this axis), these layers form a periodical structure of metal waveguides whose height smoothly varies along the radial direction from H to h.

As is known, the propagation of a plane electromagnetic wave in space would not change if one placed in its way a set of parallel ideally conducting plates directed normal to the electric field vector. In such waveguides, the wave does not differ from the plane wave in free space. Since the incidence angle of the conical plates towards the horizontal plane is quite small, the reflection from the plate system and scattering from it are insignificant. The cloaking of an object is achieved by gradual decreasing the distance between the metal plates in every effective waveguide formed by a pair of conical plates. The volume of the waveguide mode decreases in the process and it is driven out of the region wherein the distance between the plates approaches h. As a result, a diffractive wave flow takes place, similar to the one achieved in Ref. [80]. In this case, however, it is much easier to realize a cloaking device which does not contain magnetic metamaterials and, moreover, has a much broader band.

Originally, an invisibility cloak based on metal plates was designed to operate at frequencies of 3.2 ± 0.1 GHz. The dimensions of this device were electrically small (the diameter of the whole cloaking device was about the wavelength λ, and the thickness of the object to be hidden was around $0.3\,\lambda$ [77]). Later on, the parameters of the cloaking device developed were improved and a theoretical measure of cloaking of an object with a thickness of about λ was achieved at frequencies of 10.00 ± 0.25 GHz [78].

An experimental realization of such a device is presented in Ref. [79]. The following geometrical parameters were chosen for the experimental mock-up of the cloaking device (Fig. 32a): the outer diameter of the device $L_1 = 61$ mm, inner diameter $L_2 = 32$ mm, outer distance between the conical layers, $H = 9.2$ mm, spacing between the adjacent metal plates at the inner boundary of the cloaking device, $h = 6$ mm, and diameter of the hidable object (copper cylinder) $D = 30$ mm. The cloaking device consists of 20 layers (Fig. 32b). The height of the device (and of the cylinder to be hidden) amounted to 184 mm. The experiment was performed in free space, exploiting two horn antennas, one of which served as the source of electromagnetic waves, while the other was the detector. During the field scan, the receiving antenna rotated around the hidden object (Fig. 32b). It was shown that overall scattering from the system that

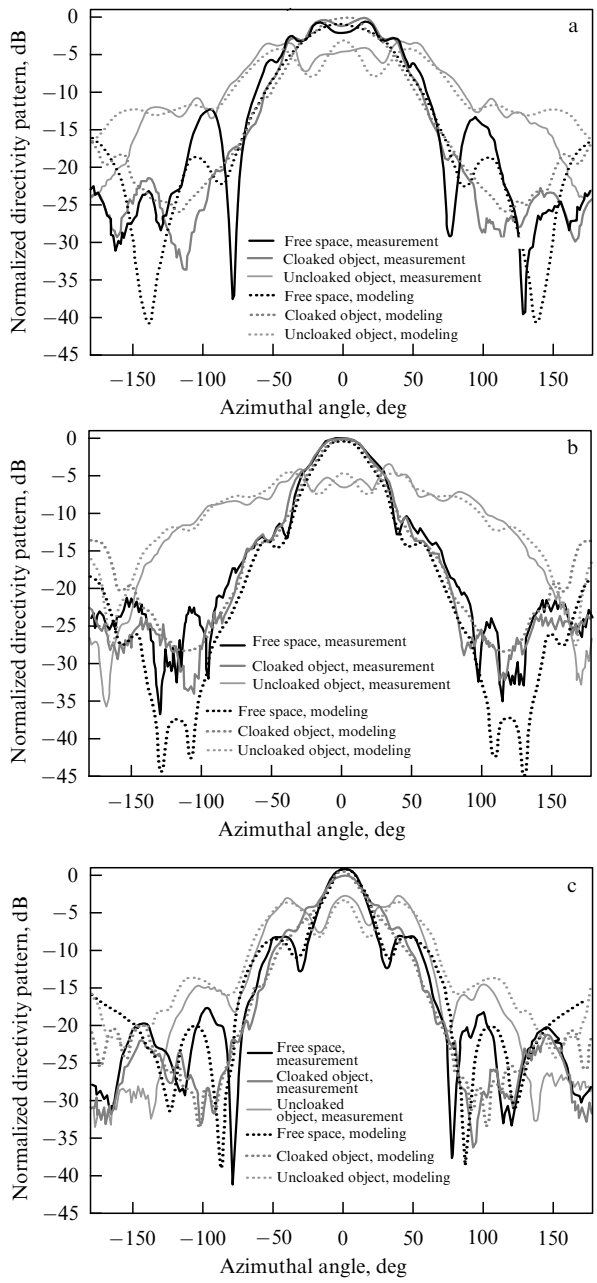

Figure 31. (Color online.) Directivity patterns at a frequency of (a) 2.5 GHz, (b) 3.0 GHz (operating frequency), and (c) 3.5 GHz [75]. The distance between the horn antenna and the center of the cloaking device is around 10 cm.

includes the cylinder with the cloaking device is reduced by 70% in comparison with the scattering from the same cylinder without the cloaking device (Fig. 32c) [79]. It was also demonstrated in Ref. [79] that such a cloaking device can suppress the scattering from the system by more than 50% in the frequency range of $\pm 20\%$.

This type of cloaking device, according to Tretyakov et al. [77], can operate not only in the microwave range, but also in the infrared range, which required using special technologies that were inaccessible to the authors of Ref. [77]. Currently, there is no experimental realization of a cloaking device based on conical metal plates that operates at optical frequencies.

2.2.3 Dielectric optical cloaking. After many attempts at fabricating cloak which would be close to ideal ones by

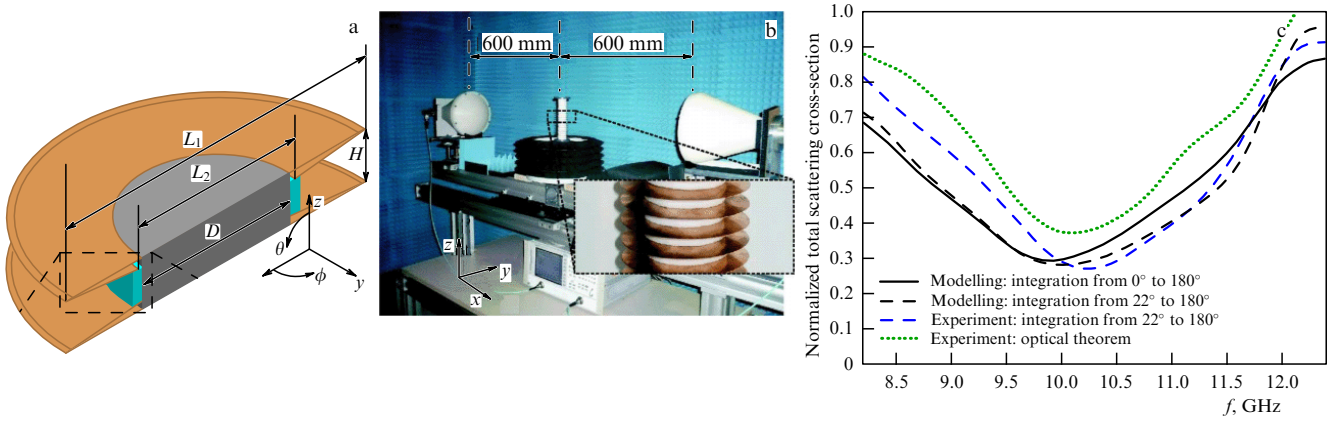

Figure 32. (a) Geometrical model of a cloaking device in the plane xy. (b) Photograph of the experimental setup for the scattering measurement (the inset shows a magnified image of the object to be hidden). (c) Results of experiment and numerical modeling for the scattering cross section of the hidden-object normalized to the scattering cross section of the original one [79].

using sophisticated metamaterials, some researchers have returned to the consideration of a nonideal invisibility cloak made of natural materials.

In article [81], the authors suggested a nonmagnetic cloaking shell based on an ordinary isotropic insulator. This device is designed for two-dimensional cloaking of the objects with a lateral size much larger than the wavelength. The density distribution of the chosen material incoming radiation with a constant permittivity ε, which would result in a strong weakening (by several times) of scattering from the hidden object, was calculated by successfully applying the method of topology optimization (a one-step method for shape and topology optimizations).

In 2013, this method of cloaking was realized experimentally [82]. A two-dimensional invisibility cloak was made of a homogeneous insulator with $\varepsilon = 2.45$ by using stereolithography and three-dimensional printing methods. The cloaking shell hides the object from several observing points, with the diameter of the inner cavity of the shell reaching 138 mm for the wavelength of 30 mm. Good results were obtained in the frequency region from 9.7 to 10.1 GHz for TE-polarization.

Based on the numerical modeling results, Urzhumov et al. [82] claim that similar results should also take place for TM-polarization, but such measurements were not performed. For TE-polarization of incident radiation at a frequency of 9.9 GHz, the scattering cross section decreases fourfold, when a cloaking shell envelops the object. The authors of the present article are sure that this method can also be applied in the optical frequency range. A photograph of the experimental sample and the measurement results are displayed in Fig. 33.

An alternative experimental realization of the dielectric unidirectional cloaking device was demonstrated in Ref. [83]. The topology optimization was performed using another method — multilevel optimization.

Paper [84] considers the possibility of exploiting not a single-layer but a multilayer dielectric cloaking shell, and a genetic algorithm was suggested in calculating the optimal value of ε for every layer (Fig. 34). It was shown theoretically

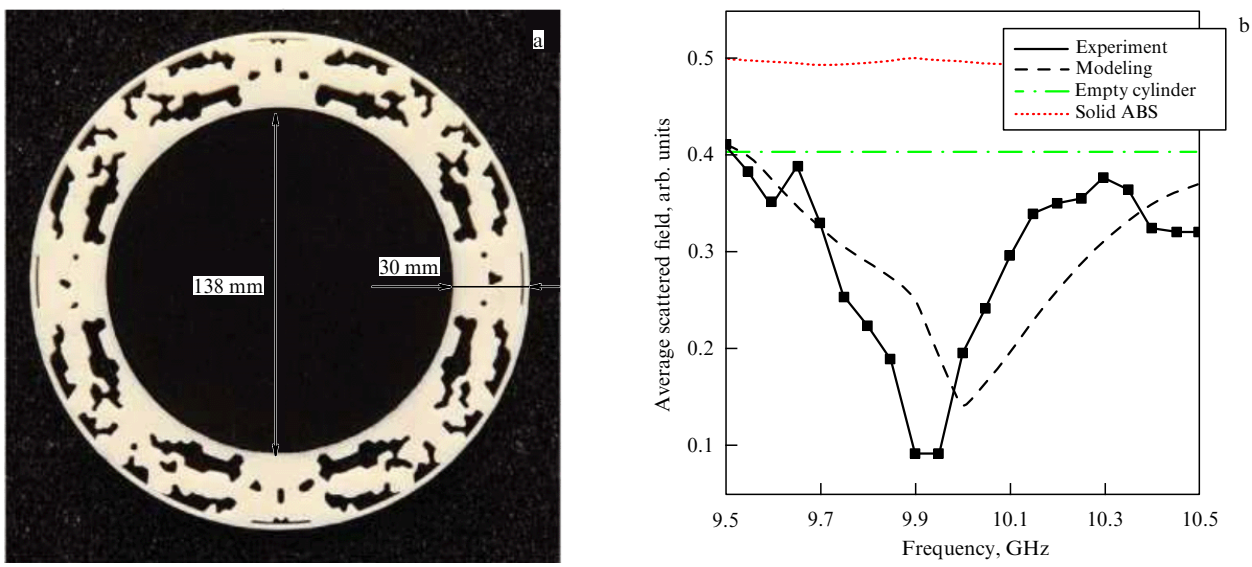

Figure 33. (a) Photograph of a dielectric cloaking shell prototype. Outer diameter of the device is 198 mm, inner is 138 mm. (b) Average scattered field in a Fresnel zone versus the incoming radiation frequency; ABS is a copolymer of acrylonitrile, butadiene, and styrene [82].

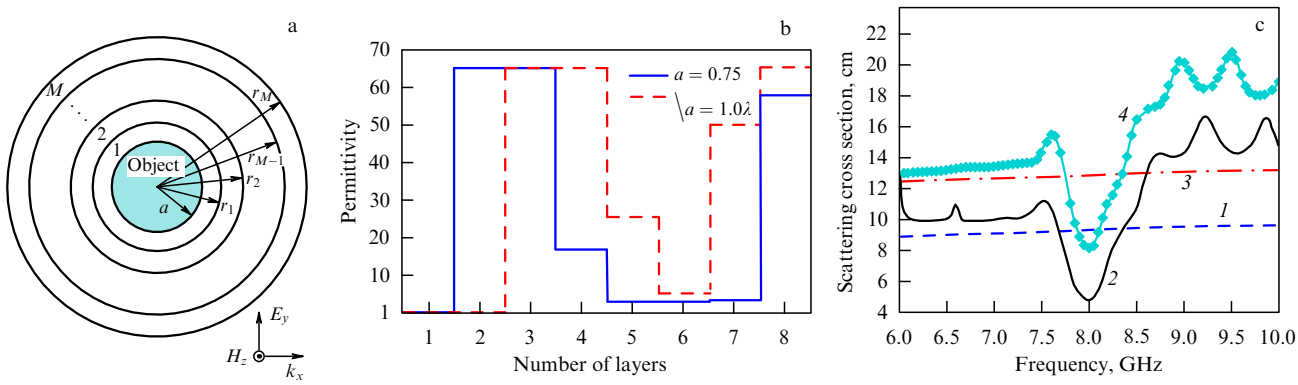

Figure 34. (a) Schematic of a multilayer dielectric invisibility cloak. (b) Permittivity of the layers obtained using the genetic algorithm. (c) Scattering cross section: *1* — original object ($a = 0.75\,\lambda$), *2* — object with cloak ($a = 0.75\,\lambda$), *3* — original object ($a = 1.0\,\lambda$), and *4* — object with cloak ($a = 1.0\,\lambda$) [84].

that such a shell with a thickness of only $0.015\,\lambda$ can decrease the scattering cross section from an object with a diameter of $1.5\,\lambda$ or $2\,\lambda$ by approximately 50%. This means that there is a way to significantly reduce the scattering from the object without utilizing metamaterials.

3. Invisibility and cloaking based on scattering cancellation

An alternative to cloaking based on the wave flow method is cloaking based on the scattering cancellation principle. This principle relies on the idea that, in order to suppress the radiation scattering from an object, one should add to it another object that would produce the scattered field possessing the same amplitude but with the opposite phase. As a result, the scattering from the system would tend to zero [85–88]. For optically small objects, which radiate as a dipole, following this cloaking procedure allows achieving invisibility for electromagnetic fields with any polarization, regardless of the radiation source and the observer's positions.

There is a significant difference between this cloaking approach and the wave flow method: the cloaked object is not isolated from the external field and it can 'see' what is going on outside and, therefore, it can serve as an ideal field sensor.

Interest in cloaking methods based on scattering cancellation has significantly increased since paper [89] was published in 2005. Currently, there are two ways of realizing this principle:

(1) by using plasmonic coatings;

(2) by using structured metal surfaces — two-dimensional analogues of metamaterials, called metasurfaces.

3.1 Cloaking based on plasmonic coatings

The idea of invisibility cloaking with the aid of the plasmonic coatings lies in placing the object into a shell made from a plasmonic material (for example, gold or silver) that has nearly zero or negative permittivity (and/or magnetic permeability). As a result, the dipole moment of the shell (or its magnetic moment) is out of phase with respect to the dipole moment vector of the object (Fig. 35) [89, 90].

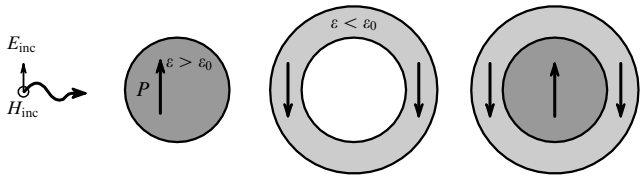

Figure 35. Cloaking principle based on plasmonic materials. The cloaking is achieved by the compensation of the object polarization, which is a result of the interaction with an electromagnetic field with the opposite polarization, induced in the plasmonic shell [89].

Plasmonic cloaking has the following advantages over other cloaking methods: it is resistant to losses in the material and the cloaked object can interact with incident radiation [89, 91–94]. Cloaking devices based on transformation optics are more sensitive to frequencies, losses in the medium, and errors caused by the invisibility cloak boundaries; moreover, the object is fully isolated in this case from the incident field and cannot be used as its sensor. A significant disadvantage of this method is the limitation imposed on the optical size of the object.

A detailed theoretical discussion of the plasmonic cloaking principle for spherical and cylindrical objects is presented in Ref. [43]. In Sections 3.1.1 and 3.1.2, we discuss the experimental realizations of this method.

3.1.1 Two-dimensional plasmonic cloaking. A two-dimensional realization of plasmonic cloaking for the microwave band was demonstrated for the first time by Edwards et al. [92]. The object to be hidden was a small rod (cylinder) made from a material with a large dielectric constant. This rod was surrounded by a plastic shell with a smaller permittivity, and the space between them was filled with acetone and metallic

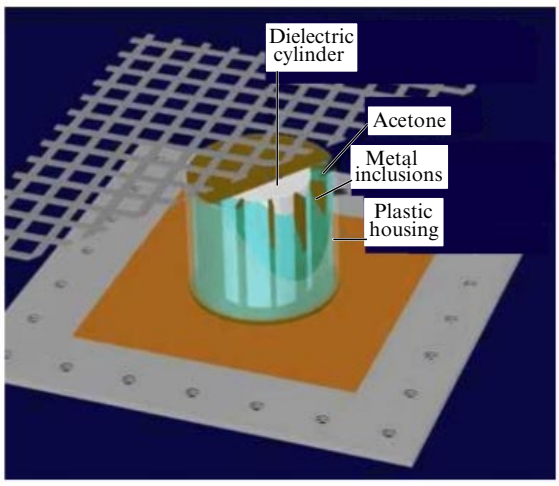

Figure 36. Schematic of the experimental setup [92].

inclusions, which provided the negative value of the dielectric constant of the shell effective medium at the operating frequency 1.93 GHz (Fig. 36). In other words, a plasmonic metamaterial, operating in the microwave band, is synthesized in the shell.

The system described above was placed in a parallel-plate waveguide, where the local-field scanner measured the electric field directed normal to the waveguide plane. The measurements were performed for three cases: for incident radiation without the object, for an uncloaked object (the space between the object and the shell in this case was filled with air), and for a cloaked object. After that, the scattering cross sections of the object (dielectric cylinder) and of the object with the plasmonic cloaking were calculated in the frequency range from 1.6 to 2.4 GHz.

Figure 37 shows a comparison of the results obtained by the analytical model, numerical modeling, and the experiment. Let us note that on every curve in Fig. 37 a significant decrease in the scattering cross section is observed, indicating its closeness to 75%. An obvious advantage of the described cloaking device lies in it easy implementation.

3.1.2 Three-dimensional plasmonic cloaking. A more interesting experimental demonstration of the plasmonic cloaking principle is the realization of three-dimensional cloaking in free space, which operates at any angle of incidence of radiation in the microwave frequency band [43, 93]. Experiment [93] was performed with a hollow dielectric cylinder, which had a small length and was covered with a thin coating of synthesized plasmonic metamaterial based on metal strips (Fig. 38). The effective dielectric constant of the cloaking shell was chosen in such a way that the scattering from the cylinder would be maximally reduced at the 3 GHz frequency for a normal incidence of the TM-polarized wave. Despite the cylindrical shape of the object and the shell, a significant scattering reduction is observed not only at normal incidence, but also at all angles of incidence and for both (TE and TM) wave polarizations. It turns out that both the object and the cloaking shell, despite their quite large dimensions in comparison with the wavelength, scatter incoming radiation at the operational frequency approximately in the same way as electric dipoles do. Their dipole polarizabilities weakly depend on the direction of the wave incidence and its polarization, just as in the case of point dipoles. As a result, one can achieve a situation where the object and the cloaking shell dipole moments approximately compensate for each other.

In order to experimentally prove the efficiency of the cloaking device performance, two independent measurement sequences were performed for a hidden object, for an original object, and for free space, and were then compared with each other. Figure 39 present the results of near-field measurements that depict show the electric field distribution along the axes of the cloaked cylinder.

Measurements of bistatic and monostatic scattering cross sections for the far-field excitation were then performed. The results are demonstrated in Figs 40, 41. Experimental results

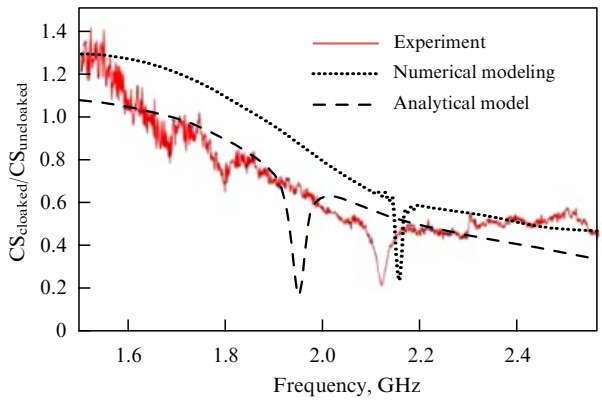

Figure 37. Ratio between widths of the scattering cross section of an object in a plasmonic cloaking shell and the scattering cross section of a uncloaked object ($CS_{cloaked}/CS_{uncloaked}$) versus the incoming radiation frequency [92].

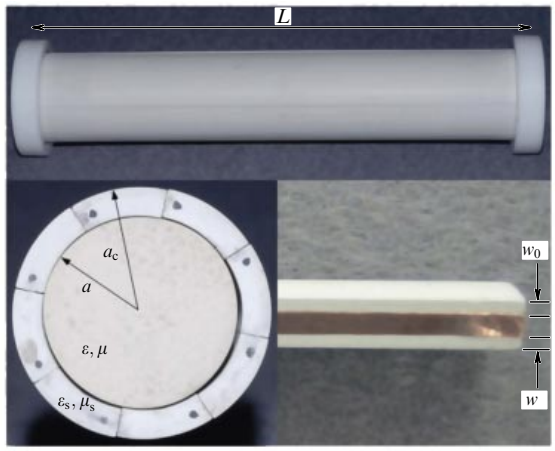

Figure 38. Experimental sample. An assembled invisibility cloak is shown in the upper part of the figure. It is in a test cylinder with caps on the edges; the length of the whole structure $L = 18$ cm. In the lower left part of the figure is the invisibility cloak cross section, where $a = 1.25$ cm, $a_c = 1.3a$. In the lower right part of the figure is the edge of the shell fragment with a copper stripe used in the fabrication of the metamaterial [93].

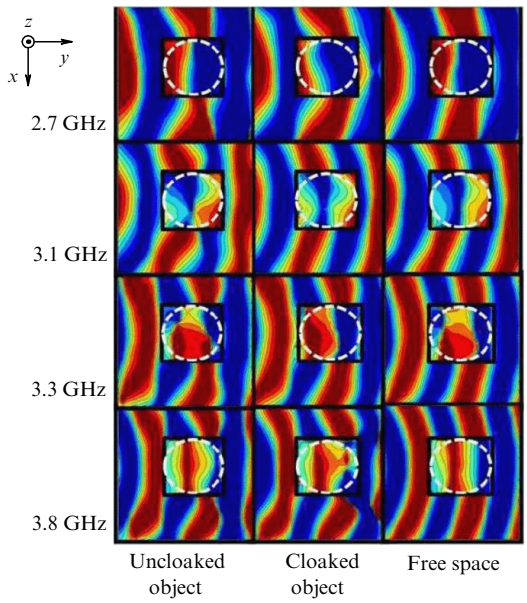

Figure 39. Near-field scanning of the electric field around and above the investigated object. First and fourth rows correspond to the frequencies at which, as expected, the cloaking does not operate well. The second row demonstrates the absence of scattering in the near field at the indicated frequency. The third row corresponds to the upper edge of the frequency band, where the cloaking effect is still observed [93].

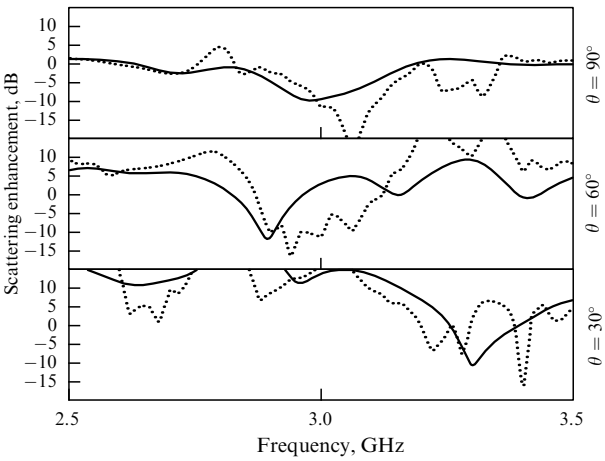

Figure 40. Monostatic scattering enhancement coefficient for a cloaked cylinder and for an uncloaked cylinder versus frequency for various angles of incidence. Numerical modeling — dotted curve, and measurement — solid curve [93].

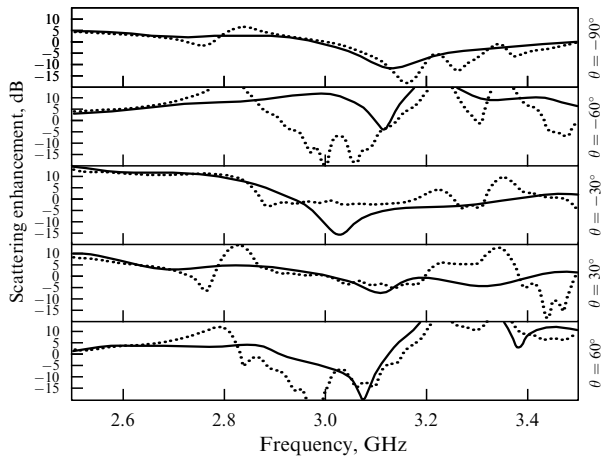

Figure 41. Bistatic scattering enhancement coefficient for various angles of radiation incidence. The numerical modeling results are shown with a dotted curve, and measurement results are plotted with a solid curve [93].

confirm that the scattering suppression is weakly sensitive to the angle of incidence of the radiation and to the observer's position and, moreover, it can be achieved in a broad frequency band.

3.2 Cloaking based on structured metasurfaces

An alternative technique for making cloaking devices based on scattering cancellation is the development of cloaking materials made of structured metal surfaces or metasurfaces. Such cloaks are also known as mantle cloaks. In this case, the scattering from the object is suppressed not by plasmonic coatings, but with surface currents that are induced on a specially synthesized metasurface. As a result, the surface current induced by the incident radiation scatters light in antiphase with the light scattered by the object, which leads to destructive interference. In order to control the scattering from the cloaking material, it is enough to create metasurfaces with a predefined surface impedance distribution.

As was shown by Chen et al. [43], synthesizing the surface impedance allows retrieval of the incident electromagnetic field distribution even near the object. The required surface impedance can be obtained not only by using metasurfaces (when the structural elements have optically small dimensions), but also by utilizing better studied (for microwave applications) frequency-selective surfaces [95]. As is known, the main difficulties that metamaterial developers meet are the narrow operational frequency band caused by the resonant nature of the metaatoms, high losses, and a required high fabrication accuracy, which is especially hard to achieve for bulk metamaterials. The mantle cloak can be quite broadband, the metasurface is much easier to fabricate than the bulk metamaterial, and, finally, resonant structure elements are not necessary in order to obtain the required surface impedance distribution.

It was shown theoretically in Refs [96–99] that, by using single-layer structures (metasurfaces or frequency-selective surfaces), a significant scattering suppression can be achieved for any angle of incidence and any polarization of the incoming wave. The frequency bandwidth of the cloaking device can be enlarged by using a metasurface with a fine structure [100–102]. The mantle cloaking can be applied both for dielectric and metal objects. However, such devices operate better with dielectric objects.

A cloaking device for the microwave region can be made of metal lattices comprising of elements with different shapes: Jerusalem crosses, sets of finite metal strips, simple crosses, etc. [95]. A monolayer of doped graphene can be used in order to achieve cloaking in the terahertz and infrared regions [103]. Metasurfaces operating in the visible light region can be created using the theory of optical nanocircuits [104].

3.2.1 Experimental realization. An experimental realization of mantle cloaking was demonstrated in Refs [105, 106] for the radio frequency range. The object to be hidden was an 18-cm long cylindrical rod with a diameter of 24.9 mm. The cloaking coating was a 'metascreen' — a layer of flexible polycarbonate film with a thickness of 100 μm, which is covered with a grid made from a 66-μm thick copper strip.

The measurement in the far field was performed for cloaked and uncloaked objects. Emitting and receiving horn antennas were located at the same distance from the object, and it was possible to move them in the azimuthal and vertical planes, as shown in Fig. 42. A significant suppression of

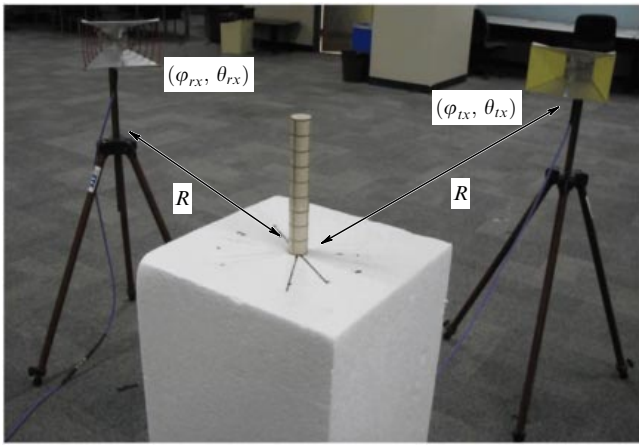

Figure 42. Experimental setup for measurements in the far field. The emitter and the receiver are located at the distance $R = 17.5\,\lambda$ from the cloaked object [105].

scattering from the cloaked object was observed in a quite broad frequency range from 1 to 5 GHz at various angles of the radiation incidence. Near-field scanning was also performed (Fig. 43). In order to scan the near-field spatial distribution around the cloaked object, a three-dimensional near-field system was exploited. Three cases were considered: without the object, with an uncloaked rod, and with a cloaked rod. As can be seen from Fig. 44, the strongest scattering suppression was observed in the frequency range from 3.3 to 3.9 GHz, and the best result was obtained on a frequency of 3.6 GHz.

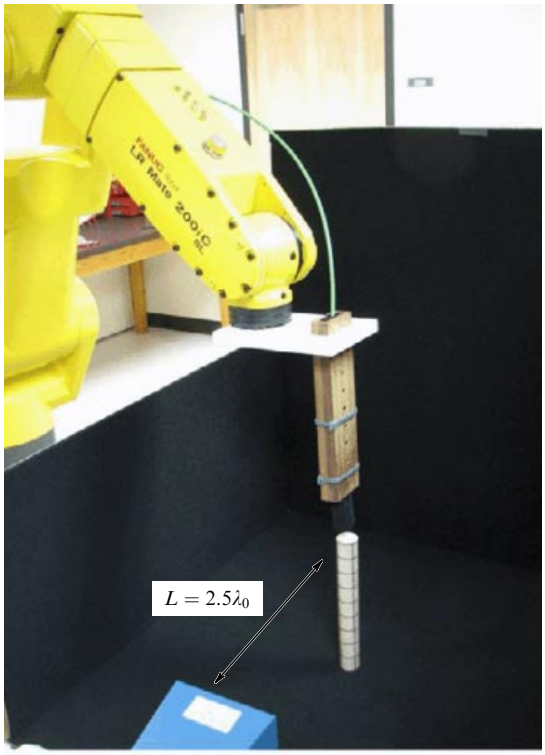

Figure 43. Experimental setup for near-field measurements [105].

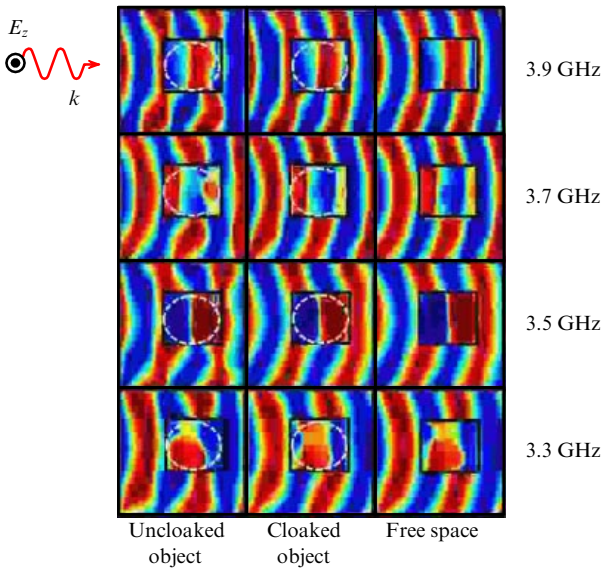

Figure 44. Electric field distribution in the azimuthal plane for various frequencies [105].

4. Other cloaking methods

4.1 Cloaking device based on lumped *LC*-elements

In 2009, the fundamental possibility of creating a cloaking device based on the circuits of lumped *LC*-elements was experimentally demonstrated [107]. A photograph of the cloaking device is shown in Fig. 45. The inductivities shorted to ground were located along the inner boundary of the device and imitated an ideal conducting cylinder — the object to be hidden. The appropriate experimental results — voltage distributions in the sample for the high radio frequencies range — are presented in Fig. 46.

4.2 Radar illusion device

The authors of paper [108] introduced a new cloaking concept based on a radar illusion device which can transform the electromagnetic image of the target, which is received by the radar, into the image of another object and mislead the enemy (Fig. 47). Such a device can be designed using transformation optics [32]. A metal cylinder is situated in real space and is surrounded by the cloaking material ('illusion cloud'), but in virtual space it is a dielectric cylinder surrounded by a vacuum. An experimental device was designed using a set of

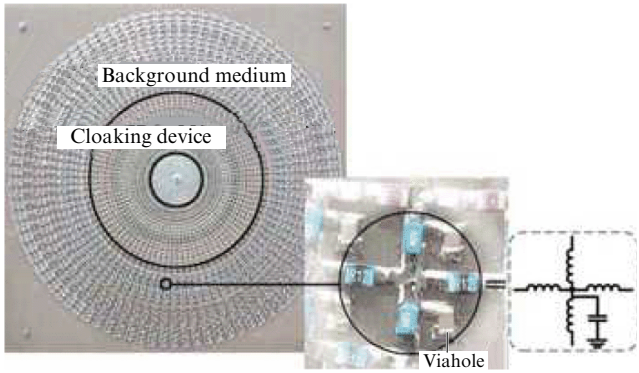

Figure 45. Photograph of a two-dimensional experimental cloaking device based on the circuits of lumped *LC*-elements [107]. The inset is a magnification of a single unit cell, consisting of four surface-mounted inductors in series and one capacitor in shunt to the ground by a via-hole.

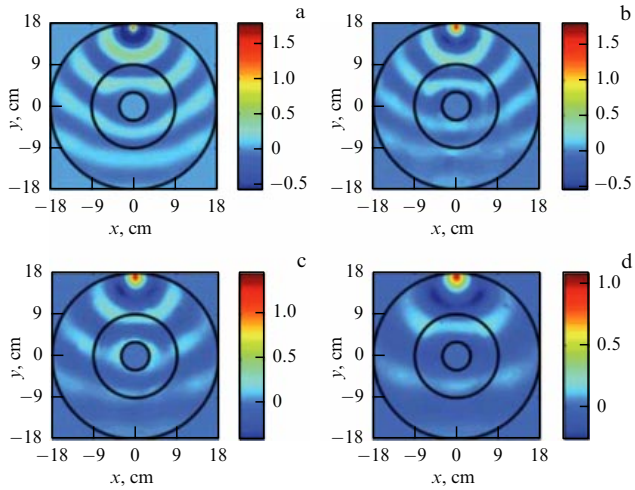

Figure 46. (Color online.) Voltage distribution in a cloaking device: (a) modeling result, and (b) measurements at the frequency of 40.1 MHz. Experimentally obtained voltage distributions on frequencies (c) 32 MHz and (d) 24 MHz [107].

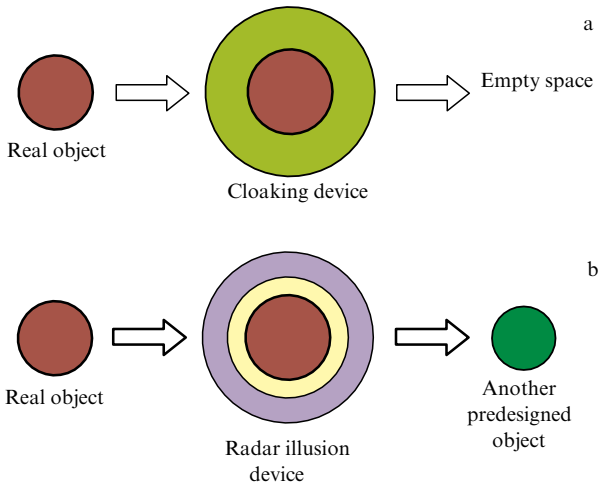

Figure 47. Illustration of the radar illusion device operation. (a) Metal object is enclosed in an ideal cloaking shell; the radar image would show nothing. (b) Metal object is placed in the illusion device; the radar image shows a virtual dielectric object [108].

SRRs that form an inhomogeneous metamaterial structure. Theoretically, this device allows the radar to be misled: the image of the metal cylinder is replaced by that of the dielectric cylinder with other dimensions.

Measurements with the radar illusion device were performed at the frequency of 9.8 GHz in a parallel-plate waveguide. The experimental results for the electric field distribution scanning, given in Fig. 48, confirm that the desired illusion effect was achieved.

The radar illusion device method was improved recently with the suggestion of a ghost cloak [109]. The main advantage of this device lies in its ability to qualitatively change the radiation scattering from the object and create its phantom images.

4.3 Active cloaking

The invisibility cloak examples discussed in Sections 1–3, 4.1, and 4.2 considered tapping materials or surfaces with specified properties. But there is another cloaking principle — *active cloaking*, wherein the object to be hidden is covered with a shell that has detectors registering the incident radiation on one side, and emitters on the other side. These emitters gather signals from the detectors and transform it into a signal that would compensate for the radiation scattering from the object and make it invisible (Fig. 49).

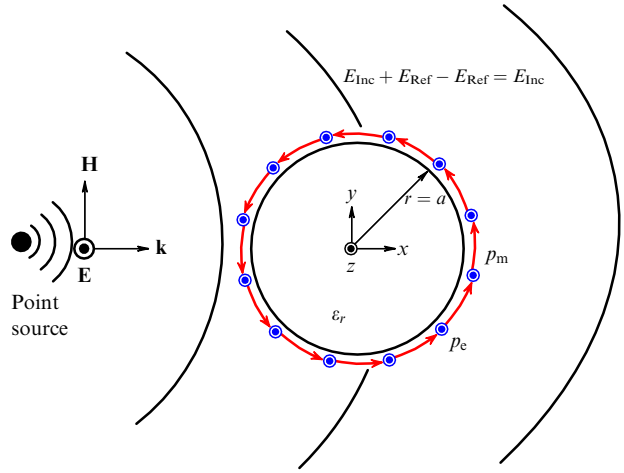

Figure 49. Active cloaking principle [112].

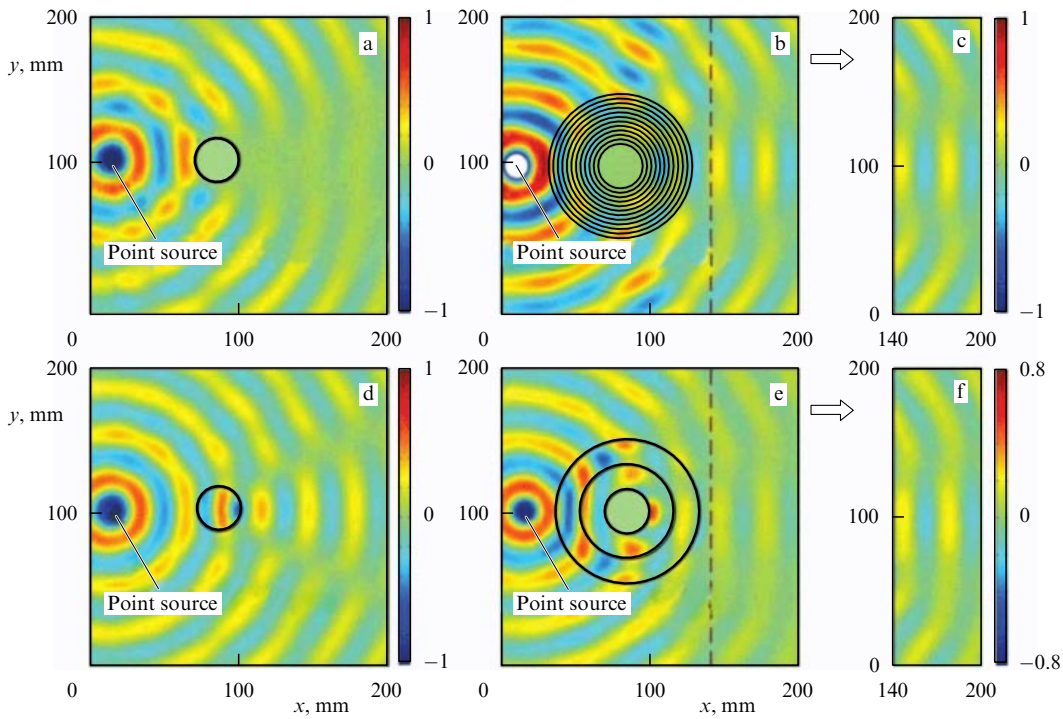

Figure 48. (Color online.) Results for a radar illusion device: (a) experiment with a copper cylinder; (b) modeling for the copper cylinder in the cloaking device; (c) modeling results that show the electric field distribution behind the device; (d) experiment with a dielectric cylinder; (e) experiment with the copper cylinder inside the cloaking device, and (f) experimental results showing the electric field distribution behind the device [108].

Thus, any object with known electromagnetic properties can be cloaked in this way by adjusting the signal from the cloaking shell emitters. This type of cloaking was first suggested for acoustic waves [26, 110], because active cloaking requires that the spatial field distribution be known in order to compensate for the scattering by the cloaking shell sources. In the case of slowly propagating waves, the information can be transmitted inside the cloaking shell with a higher speed, leaving time for the calculation of the optimal signal for every emitter. As a result, the required compensation signal would appear in time and the object would be impossible to detect. Active cloaking can be applied to electromagnetic waves in a vacuum if one knows the parameters of the incident radiation and the properties of an object scattering. This allows predefining the characteristics of the field which is built by the cloaking shell sources [26].

Miller [26] also discussed in his paper the possibility of active cloaking realization when there is no information about the incoming radiation field and one has to analyze it in real time and calculate the compensating radiation. However, this realization appears to be difficult to manage, because the distribution calculation time needs to be less than the propagation time for the electromagnetic wave in the cloaking shell. That is why there were no realizations of active cloaking before 2013.

In November 2013, two studies of different groups were published almost simultaneously [111, 112]. They demonstrated experimental realizations of the active cloaking shells for the microwave frequency band. In both cases, the source of the electromagnetic waves was predefined and the experimental results were in good agreement with the numerical modeling. Moreover, it was argued that this concept can also be applied to create illusions.

4.4 Optical illusions

For a long time, illusionists have been tapping various optical illusions to mislead an audience with their tricks. The secret of such tricks is quite easy: one needs just to build up an optical setup using ordinary mirrors and lenses in such way that the rays reflect at a proper angle. The same principle is used in a 'sham X-ray apparatus' (Fig. 50), which was invented in the 20th century, and a periscope utilized on submarines [113]. The optical illusion effect (or the reality misperception effect) is in some way an alternative to invisibility. Moreover, currently there are a number of studies that are devoted precisely to optical illusions, which look at first sight like the invisibility effect.

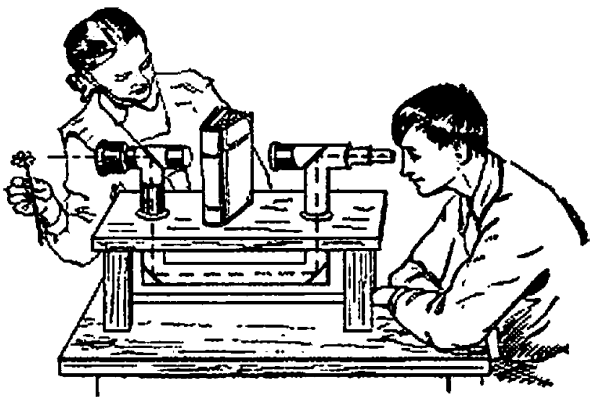

Figure 50. A sham X-ray apparatus [113].

Figure 51. 'Invisibility cloak' which creates an optical illusion of transparency. © Tachi Laboratory Graduate School of Media Design, Keio University.

One example of an optical camouflage is demonstrated by a group of Japanese scientists under the guidance of S Tachi [114]. The scientists have developed a so-called transparent invisibility cloak. Its cloth reproduces the image of objects which are located on the opposite side of the cloak (Fig. 51). Therefore, if one looks at person dressed in this cloak, it will seem that the person is transparent, and it does not matter whether the person is observed from the front or from the back.

The secret of this invisibility cloak lies in the fact that it consists of glass beads with built-in mini-cameras. The cameras film everything which is happening in the front and then transmit the image to the other side of the cloak, and vice versa. Of course, this retro-reflective projection technology is not perfect and needs to be improved, but as the developers say, it would be useful for the construction of airplanes with transparent cabins and in the automobile industry.

Since the eyesight of most animals, including humans, is not sensitive to polarization and phase of the light, they do not have to be taken into account in cloaking device development, which makes it an easier task. This consideration was taken advantage in Ref. [115]. In the experiments demonstrated, the cloaking device was a set of glass lenses with the refraction index $n = 1.78$, glued to each other in a specific way. In the first experiment (Fig. 52), a hexagonal cloaking device was placed in an aquarium with water, and a goldfish played the role of a cloaked object. As soon as the fish enters the cloak, it becomes invisible to the human eye, and everything which is situated behind it continues to be visible. The cloaking device itself is slightly noticeable to the eye, due to remainders of glue on the lens faces with a refractive index somewhat different from that of water. Such a cloaking device operates at six different view angles.

In the second experiment (Fig. 53), the cloaked object was a cat, and the hexagonal setup was replaced with a tetragonal one. The lens system is placed in front of the screen, and a video with a flying butterfly is projected on it. When the cat is brought into the cloaking device, it disappears, but the butterfly can still be seen. Such a cloaking device can operate for four light propagation directions, although in this experiment it had only one direction.

Another example of an optical illusion is a mirage emergence in the desert, which occurs as a result of troposphere refraction (a light beam bends in nonuniformly heated air). In this case, the person can see a pond at the place where

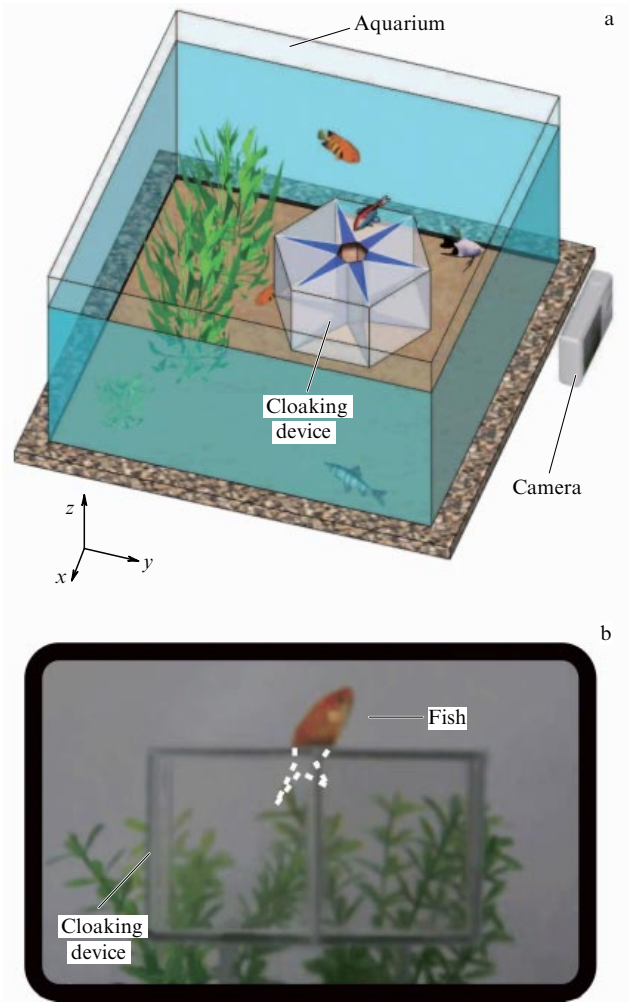

Figure 52. Experimental observation of a fish hiding in an aquarium [115].

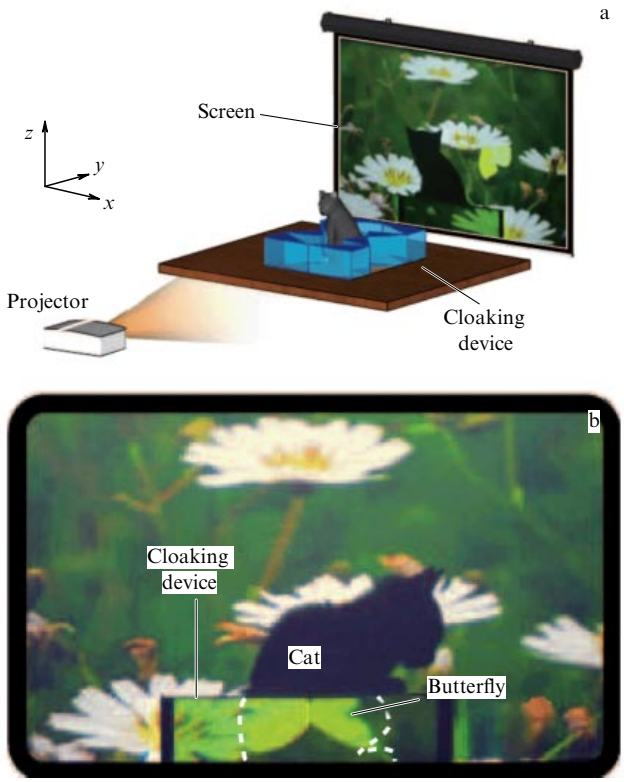

Figure 53. Experimental observation of a cat hiding behind a screen in the grass [115].

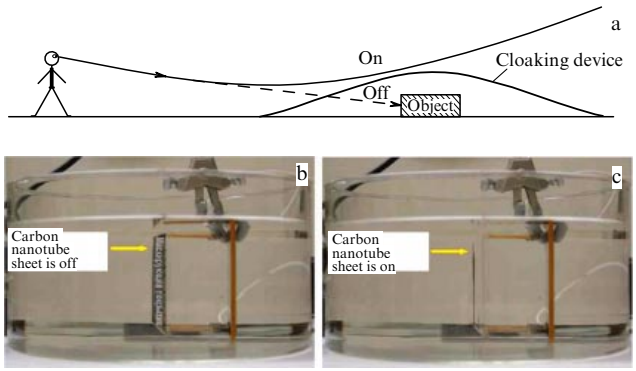

Figure 54. (a) Schematic representation of a cloaking system. (b,c) Mirage effect under water [116].

it is absent, because the objects seem to be below the horizon and inverted due to troposphere refraction. This looks the same as when objects are reflected in water. On the other hand, the light scattered by the object in the direction of the observer can bend around him due to troposphere refraction. Hence, the object placed within the line of sight would become invisible.

A principle similar to troposphere refraction is the cloaking method based on the photothermal deflection effect of a light beam propagating in composite media. This principle was experimentally verified in work [116]. A three-dimensional array of carbon nanotubes possessing a low heat capacity and high thermal conductivity causes a large modulation frequency of the temperature, and hence causes sharp spatial changes to the refractive index of such a metamaterial. In the experiment, shown in Fig. 54, an array of nanotubes was placed in water and the cloaked object (designated as 'cloaking device') is placed on the side face of the glass container. The nanotube metamaterial was resistively heated, which resulted in almost complete invisibility of the sign and the tubes themselves. The array responded in several seconds to the heating turning on or off. The refractive index of the array of nanotubes can also be controlled by using electromagnetic pulses. This creates a refractive index gradient which allows deflecting the light beam in a very broad wavelength range from UV to IR.

Cloaking devices which rely in their operation on known laws of geometrical optics are demonstrated in Ref. [117]. These devices allow hiding any objects with dimensions that do not exceed 10^6 mm^3; the biggest volume which has successfully been cloaked amounts to 10^8 mm^3. There are three different versions of such a cloaking device. The first one was based on Snell's law and consisted of two L-shaped reservoirs filled with water in order for light to refract around the cloaked region. The first lens creates a parallel light beam, so the rays bend around the cloaked region, and the second lens gathers these rays together afterwards. This means that any object that is placed in the space between the reservoirs is hidden from the human eye (a toy helicopter was successfully cloaked in Ref. [117]). The main disadvantage is that only that part of the object which reaches the water level is cloaked. There is no artificial light refraction above this level, and the upper part of the object will be visible. The second device,

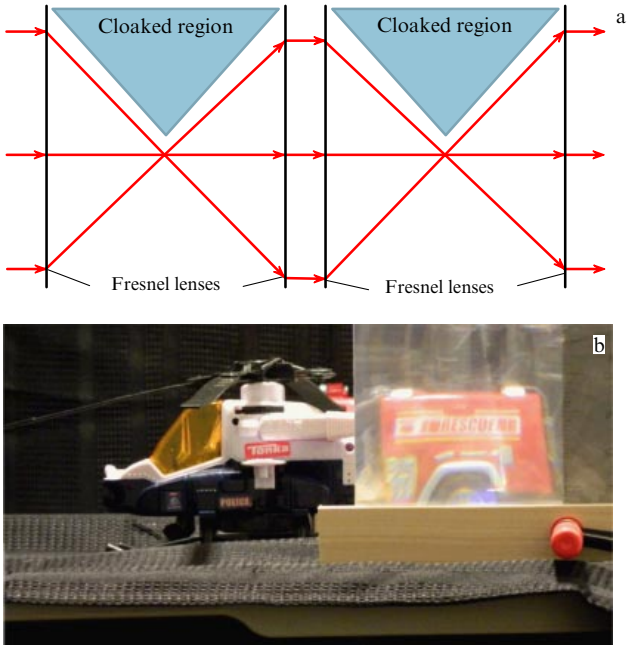

Figure 55. Cloaking with lenses. (a) Schematic of the setup: two pairs of Fresnel lenses with double focal length spacing prevent the inversion of the image. The distance between the lens pairs can be arbitrarily small. In the real experiment, they were mounted together as if there was one lens. (b) The image along the optical axis: a truck appears instead of the helicopter tail. The photograph is made with a 21x zoom at a distance of 6.4 mm from the first lens [117].

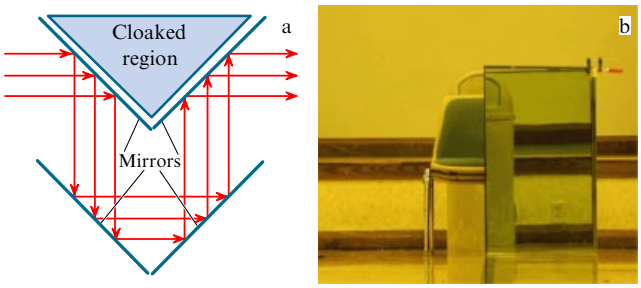

Figure 56. Cloaking with mirrors: (a) schematic of the experimental setup, and (b) experimental confirmation: part of a chair, located between mirrors, is hidden, and instead of it we see the garbage container [117].

demonstrated in Fig. 55a, consists of Fresnel lenses which direct the light in such a way that it bends around the cloaked region and there is no edge effect as in the first case. In a similar way, mirrors are used with the same purpose of light bending around the object in the third method (Fig. 56). The system consisted of four mirrors: two pairs oriented perpendicular to each other. One mirror reflects the light from the cloaked region, and the other three guide the light out of it. Indisputable advantages of all these devices are their ability to cloak sufficiently large three-dimensional objects, fabrication simplicity, and ability to operate in the optical range.

Of course, none of these optical illusions falls under the definition of invisibility. An object can be detected by using special measurements, and not only by the eye. Scattered radiation fields can also be detected through phase (interference) measurements, and all optical illusions can be 'exposed' by performing them. We discuss these studies only in order to emphasize the difference between the invisibility illusion and optical invisibility proper, even if it is not ideal.

One should also note another cloaking principle, which is related exactly to invisibility, but yet has had no extensive development or experimental confirmation — the external cloaking principle. This principle assumes that there is some object which creates an 'invisibility region' around itself. As soon as other objects enter this area, they also become invisible [27].

5. Limitations of cloaks

There are fundamental limitations on the operation of cloaking materials based both on the wave flow method and on the scattering cancellation principle.

The first limitation is related to the *superluminal propagation of light*. Electromagnetic waves that propagate through a cloaking device, as shown in Fig. 1a, travel at distances which are longer than the ones they would have passed if they were propagating in free space. In order for the optical path of the beam, defined as $\int n\,\mathrm{d}l$, inside the cloaking device to be the same as that of the rays in a vacuum (it is necessary for the wave front to be recovered after the object), the velocity of the electromagnetic wave in the invisibility cloak needs to be more than the speed c of light in vacuum. The phase speed of the wave can exceed c if the refractive index of the cloaking medium is less than one. But, first, it is not easy to fabricate such media in a solid state. Second, the propagation speed of an electromagnetic wave energy, as well as the group velocity of the pulse signal, cannot exceed c. Therefore, an object cannot be hidden in a cloaking shell made of a material with a refractive index of less than unity.

It should be noted that this limitation is absent for acoustic waves, so the problem of acoustic cloaking can be solved more easily. For electromagnetic, including optical, cloaking this limitation is not fundamental if the cloaked object is only located in a medium with a high refractive index. In this case, cloaking material can be made of a less optically dense medium. However, most of the practical applications require object cloaking precisely in air, where the speed of light is actually c. In order to realize such cloaks, the gain media have been suggested — substances exhibiting population inversion of energy levels [50], as well as the structures based on non-Euclidean transformation optics [118]. In both these cases, the geometry-optical pattern of the wave flow, shown in Fig. 1a, is not quite suitable. The recovery of the wave front behind the object takes place due to specially synthesized diffraction. However, both these approaches are hard to realize experimentally. For example, invisibility cloaks based on non-Euclidean transformation optics have to be fabricated using a material with quite large ε (around 1000). Additionally, the larger the area we want to hide, the higher the required value of ε [118], which is really hard to realize in the practice.

Strictly speaking, the realization of diffractive recovery for a wave front behind the object does not necessarily need non-Euclidean geometry. Therefore, in 2012, a two-dimensional optical cloaking (i.e., cloaking of cylindrical objects under the requirement that electromagnetic waves propagate normal to the cylinder axis) was realized [80]. The invisibility cloak was formed by a cylindrical shell made of an anisotropic metamaterial with magneto-dielectric properties. The permittivity tensor components of the metamaterial varied from 1 on the outer surface of the shell to 40 on the inner side, while the magnetic permeability tensor components varied from 1

on its outer surface to 0.18 on the inner one. Although in geometry-optical approximation the rays should propagate inside the shell with a speed of more than c, and the wavefront of the transmitted field should be distorted, but actually geometrical optics approach does not stand true in this case and the transmitted field demonstrates the recovery of the wavefront. This effect occurs due to the right choice of not only the radial dependence of the metamaterial electromagnetic parameters, but also the metamaterial shell thickness which determines the diffraction regime. Let us note that this regime is resonant, so the cloaking of the inner cylinder in work [80] was achieved in a rather narrow bandwidth.

Another problem of experimental realization of invisibility cloaks is related to *the correct calculation of effective electromagnetic parameters of the metamaterial* which will be chosen for the cloaking. Precise numerical calculation of a cloaking device made of a metamaterial containing a very large number of metaatoms is possible in the best case only once — that is, for one set of particle array parameters. Even single precise calculation needs a vast computing resource. Therefore, the optimization of the cloaking material is performed in the framework of the effective medium approximation. This means that the metamaterial constituting the invisibility cloak is assumed to be a continuous medium and is described in terms of dielectric constant and magnetic permeability. This analytical model of the metamaterial is known as the homogenization model and has a limited scope of application.

Unfortunately, the applicability limitations of known homogenization models require the effective medium to be almost homogeneous, meaning that the distances between the metamaterial particles, their shape, and their size weakly vary along any direction. However, in order to make a cloaking device, one needs to vary the permittivity and magnetic permeability of the medium on scales less than the incoming radiation wavelength. In other words, unlike usual metamaterials, particle arrays that realize the invisibility cloak need to be aperiodic with predefined variations of both the interparticle distances and sometimes the particle geometry. Therefore, scales at which ε and μ of the effective medium need to vary turn out to be comparable with the interparticle distance, so the homogenization model used for the development of cloaking materials seems to be evidently incorrect. The fact that the working model is inadequate turns the development of cloaking devices into some kind of art. Although the invisibility cloaks synthesized with the aid of the homogenization model from real artificial particles are always tested by precise numerical simulations, the inconsistency of the model itself inevitably questions the success of the final result. We believe that this is the main reason for the fact that experimental realizations of cloaking devices, despite significant financing of this work, do not correspond to the progress in theory, especially for the optical range.

6. Conclusion

This article presents a review of experimental realizations of cloaking devices, which allow achieving to some extent the effect of optical (electromagnetic) invisibility of objects. The two most common principles are described in detail: wave flow and scattering cancellation. Each method of optical (electromagnetic) cloaking has its own advantages and disadvantages that determine the principle which is more suitable for specific applications. The wave flow-assisted cloaking theoretically allows hiding objects of any shape and of quite large dimensions with respect to the operating wavelength. In most cases, however, these devices are narrowband and are very sensitive to optical losses and to the manufacturing precision of the elements. Other cases of broadband and quite stable cloaking devices offer only two-dimensional cloaking or cloaking under a 'transparent carpet', when the cloaking device itself is visible.

On the other hand, cloaking devices based on scattering cancellation turn out to be less sensitive to the manufacturing precision of the structure and to have a much broader frequency band, but the dimensions of the object cannot exceed the incoming radiation wavelength.

The maximum size of an object which was successfully hidden in the experiment from electromagnetic fields using the wave flow method is currently six wavelengths [82]. The perfect invisibility has not been achieved. However, it should be noted that researchers have significantly advanced in this field in comparison with the first realization of the cloaking device in 2006, at least in the microwave band.

Acknowledgments
The authors are grateful to N N Rozanov and Y S Kivshar for the fruitful discussions. The study was partly financed by the Russian Federation Government (grant 074-U01, contract 11.G34.31.0020), the Russian Foundation for Basic Research, and the Dynasty fund.

References

1. Jacobs J *English Fairy Tales* (London: David Nutt, 1890)
2. Rowling J K *Harry Potter and the Philosopher's Stone* (London: Bloomsbury, 1997)
3. Wells H G *The Invisible Man* (London: C. Arthur Pearson, 1897)
4. Slyusar V *Elektronika NTB* (7) 70 (2009)
5. Vendik I B, Vendik O G *Tech. Phys.* **58** 1 (2013); *Zh. Tekh. Fiz.* **83** (1) 3 (2013);
6. Lapine M, Tretyakov S *IET Microwaves Antennas Propag.* **1** 3 (2007)
7. Shalaev V M *Nature Photon.* **1** 41 (2007)
8. Sarychev A K, Shalaev V M *Electrodynamics of Metamaterials* (Singapore: World Scientific, 2007)
9. Solymar L, Shamonina E *Waves in Metamaterials* (Oxford: Oxford Univ. Press, 2009)
10. Noginov M A, Podolskiy V A (Eds) *Tutorials in Metamaterials* (Boca Raton, Fl.: Taylor and Francis, 2012)
11. Engheta N, Ziolkowski R W (Eds) *Metamaterials: Physics and Engineering Explorations* (Hoboken, NJ: Wiley-Interscience, 2006)
12. Capolino F (Ed.) *Theory and Phenomena of Metamaterials* (Boca Raton, Fl.: CRC Press/Taylor and Francis, 2009)
13. Capolino F (Ed.) *Applications of Metamaterials* (Boca Raton, Fl.: CRC Press, 2009)
14. Cui T J, Smith D R, Liu R (Eds) *Metamaterials: Theory, Design, and Applications* (New York: Springer, 2010)
15. Zouhdi S, Sihvola A, Vinogradov A P (Eds) *Metamaterials and Plasmonics: Fundamentals, Modelling, Applications* (Dordrecht: Springer, 2009)
16. Cai W, Shalaev V *Optical Metamaterials: Fundamentals and Applications* (New York: Springer, 2010)
17. Veselago V G *Phys. Usp.* **54** 1161 (2011); *Usp. Fiz. Nauk* **181** 1201 (2011)
18. Rozanov N N *Priroda* (6) 3 (2008)
19. Wolf E, Habashy T *J. Mod. Opt.* **40** 785 (1993)
20. Monticone F, Alù A *Phys. Rev. X* **3** 041005 (2013)
21. Kildishev A V, Shalaev V M *Phys. Usp.* **54** 53 (2011); *Usp. Fiz. Nauk* **181** 59 (2011)
22. Maier S A *Plasmonics: Fundamentals and Applications* (New York: Springer, 2007)

23. Klimov V V *Nanoplazmonika* (Nanoplasmonics) (Moscow: Fizmatlit, 2010)
24. Ufimtsev P Ya *Metod Kraevykh Voln v Fizicheskoi Teorii Difraktsii* (Method of Edge Waves in the Physical Theory of Diffraction) (Moscow: Sovetskoe Radio, 1962)
25. Ufimtsev P Y *Theory of Edge Diffraction in Electromagnetics* (Raleigh, NC: SciTech, 2009)
26. Miller D A B *Opt. Express* **14** 12457 (2006)
27. Nicorovici N P et al. *Opt. Express* **15** 6314 (2007)
28. Alitalo P, Tretyakov S *Proc. IEEE* **99** 1646 (2011)
29. Dubinov A E, Mytareva L A *Phys. Usp.* **53** 455 (2010); *Usp. Fiz. Nauk* **180** 475 (2010)
30. Rozanov N N *Phys. Usp.* **54** 763 (2011); *Usp. Fiz. Nauk* **181** 787 (2011)
31. Dubinov A E, Mytareva L A *Phys. Usp.* **55** 315 (2012); *Usp. Fiz. Nauk* **182** 337 (2012)
32. Pendry J B et al. *Science* **312** 1780 (2006)
33. Leonhardt U *Science* **312** 1777 (2006)
34. Leonhardt U *New J. Phys.* **8** 118 (2006)
35. Leonhardt U, Philbin T G *New J. Phys.* **8** 247 (2006)
36. Dolin L S *Izv. Vyssh. Uchebn. Zaved. Radiofiz.* **4** 964 (1961)
37. Dantzig D V *Proc. Cambr. Philos. Soc.* **30** 421 (1934)
38. Lax M, Nelson D F *Phys. Rev. B* **13** 1777 (1976)
39. Post E J *Formal Structure of Electromagnetics: General Covariance and Electromagnetics* (New York: Interscience Publ., 1962)
40. Ward A J, Pendry J B *J. Mod. Opt.* **43** 773 (1996)
41. Teixeira F L, Chew W C *J. Math. Phys.* **40** 169 (1999)
42. Teixeira F L, Chew W C *J. Electromag. Waves Appl.* **13** 665 (1999)
43. Chen P Y et al. *Adv. Mater.* **24** OP281 (2012)
44. Schurig D et al. *Science* **314** 977 (2006)
45. Kundtz N, Gaultney D, Smith D R *New J. Phys.* **12** 043039 (2010)
46. Kanté B, Germain D, de Lustrac A *Phys. Rev. B* **80** 201104(R) (2009)
47. Guven K et al. *New J. Phys.* **10** 115037 (2008)
48. Vozianova A V, Khodzitskii M K *Nauch.-Tekh. Vestn. Inform. Tekhnol. Mekh. Opt.* (4) 28 (2012)
49. Semouchkina E et al. *Appl. Phys. Lett.* **96** 233503 (2010)
50. Greenleaf A et al. *Commun. Math. Phys.* **275** 749 (2007)
51. Karpov I A, Shoo E D *Rev. Sci. Instrum.* **83** 074704 (2012)
52. Kante B et al. *Opt. Express* **16** 6774 (2008)
53. Li J, Pendry J B *Phys. Rev. Lett.* **101** 203901 (2008)
54. Liu R et al. *Science* **323** 366 (2009)
55. Zhou F et al. *Sci. Rep.* **1** 78 (2011)
56. Ergin T et al. *Science* **328** 337 (2010)
57. Bao D et al. *New J. Phys.* **13** 103023 (2011)
58. Ma H F, Cui T J *Nature Commun.* **1** 21 (2010)
59. Shin D et al. *Nature Commun.* **3** 2013 (2012)
60. Landy N, Smith D R *Nature Mater.* **12** 25 (2012)
61. Liang D et al. *Adv. Mater.* **24** 916 (2012)
62. Valentine J et al. *Nature Mater.* **8** 568 (2009)
63. Gharghi M et al. *Nano Lett.* **11** 2825 (2011)
64. Fischer J et al. *Opt. Lett.* **36** 2059 (2011)
65. Ergin T, Fischer J, Wegener M *Phys. Rev. Lett.* **107** 173901 (2011)
66. Narayana S, Sato Y *Adv. Mater.* **24** 71 (2012)
67. Gomory F et al. *Science* **335** 1466 (2012)
68. Schittny R et al. *Phys. Rev. Lett.* **110** 195901 (2013)
69. Xu H et al. *Phys. Rev. Lett.* **112** 054301 (2014)
70. Han T et al. *Phys. Rev. Lett.* **112** 054302 (2014)
71. Schittny R et al. *Science* **345** 427 (2014)
72. Stenger N, Wilhelm M, Wegener M *Phys. Rev. Lett.* **108** 014301 (2012)
73. Alitalo P et al. *IEEE Trans. Antennas Propag.* **56** 416 (2008)
74. Alitalo P et al. *Appl. Phys. Lett.* **94** 014103 (2009)
75. Vehmas J et al. *IET Microw. Antennas Propag.* **6** 830 (2012)
76. Alitalo P et al. *IET Trans. Antennas Propag.* **60** 4963 (2012)
77. Tretyakov S et al. *Phys. Rev. Lett.* **103** 103905 (2009)
78. Alitalo P, Tretyakov S A *Phys. Rev. B* **82** 245111 (2010)
79. Alitalo P et al. *J. Appl. Phys.* **111** 034901 (2012)
80. Xu S et al. *Phys. Rev. Lett.* **109** 223903 (2012)
81. Andkjær J, Sigmund O *Appl. Phys. Lett.* **99** 021112 (2011)
82. Urzhumov Y et al. *Opt. Lett.* **38** 1606 (2013)
83. Lan L et al. *Appl. Phys. Lett.* **103** 121113 (2013)
84. Wang X, Semouchkina E *Appl. Phys. Lett.* **102** 113506 (2013)
85. Kerker M *J. Opt. Soc. Am.* **65** 4 376 (1975)
86. Kahn W K, Kurss H *IEEE Trans. Antennas Propag.* **13** 671 (1965)
87. Chew H, Kerker M *J. Opt. Soc. Am.* **66** 445 (1976)
88. Sihvola A "Properties of dielectric mixtures with layered spherical inclusions", in *Microwave Radiometry and Remote Sensing Applications* (Ed. P Pampaloni) (Boca Raton, Fl.: CRC Press, 1989)
89. Alù A, Engheta N *Phys. Rev. E* **72** 016623 (2005)
90. Alù A, Engheta N *Phys. Rev. Lett.* **100** 113901 (2008)
91. Alù A, Rainwater D, Kerkhoff A *New J. Phys.* **12** 103028 (2010)
92. Edwards B et al. *Phys. Rev. Lett.* **103** 153901 (2009)
93. Rainwater D et al. *New J. Phys.* **14** 013054 (2012)
94. Filonov D et al. *Phys. Status Solidi RRL* **6** 46 (2012)
95. Munk B A *Frequency Selective Surface: Theory and Design* (New York: Wiley, 2000)
96. Alù A *Phys. Rev. B* **80** 245115 (2009)
97. Chen P-Y, Alù A *Phys. Rev. B* **84** 205110 (2011)
98. Chen P-Y et al. *IEEE Antennas Propag. Lett.* **5** 1598 (2011)
99. Chen P-Y, Alù A *ACS Nano* **5** 5855 (2011)
100. Alù A, Engheta N *Phys. Rev. E* **72** 016623 (2005)
101. Kallos E et al. *Phys. Rev. B* **84** 045102 (2011)
102. Alitalo P et al. *J. Appl. Phys.* **107** 034905 (2010)
103. Engheta N, Salandrino A, Alù A *Phys. Rev. Lett.* **95** 095504 (2005)
104. Engheta N *Science* **317** 5845 (2007)
105. Soric J C et al. *New J. Phys.* **15** 033037 (2013)
106. Soric J C et al. *Proc. IEEE Antennas Propag. Soc. Int. Symp.* (1 – 2) (2012)
107. Liu X et al. *Appl. Phys. Lett.* **95** 191107 (2009)
108. Jiang W X, Cui T J *Phys. Rev. E* **83** 026601 (2011)
109. Jiang W X et al. *Adv. Func. Mater.* **23** 4028 (2013)
110. Nelson P A, Elliott S J *Active Control of Sound* (New York: Academic Press, 1992)
111. Ma Q et al. *Phys. Rev. Lett.* **111** 173901 (2013)
112. Selvanayagam M, Eleftheriades G V *Phys. Rev. X* **3** 041011 (2013)
113. Perelman Ya I *Zanimatel'naya Fizika* (Physics for Entertainment) Book 1 (Moscow: Nauka, 1979)
114. Tachi Lab Projects, Retro-reflective Projection Technology, http://www.tachilab.org/modules/projects/rpt.html
115. Chen H et al. *Nature Commun.* **4** 1 (2013)
116. Aliev A E, Gartstein Yu N, Baughman R H *Nanotechnology* **22** 435704 (2011)
117. Howell J C et al. *Appl. Opt.* **53** 9 1958 (2014)
118. Perczel J, Tyc T, Leonhardt U *New J. Phys.* **13** 083007 (2011)